DOI: 10.1534/genetics.109.104497

Polymorphisms in Multiple Genes Contribute to the Spontaneous Mitochondrial Genome Instability of *Saccharomyces cerevisiae* S288C Strains

Lazar N. Dimitrov,*,† Rachel B. Brem,‡ Leonid Kruglyak§ and Daniel E. Gottschling*,†,[1]

**Department of Genome Sciences, University of Washington, Seattle, Washington 98195, ‡Department of Molecular and Cell Biology, University of California, Berkeley, California 94720, §Lewis-Sigler Institute for Integrative Genomics, Department of Ecology and Evolutionary Biology and Howard Hughes Medical Institute, Princeton University, Princeton, New Jersey 08544 and †Division of Basic Sciences, Fred Hutchinson Cancer Research Center, Seattle, Washington 98109*

Manuscript received April 28, 2009
Accepted for publication July 1, 2009

ABSTRACT

The mitochondrial genome (mtDNA) is required for normal cellular function; inherited and somatic mutations in mtDNA lead to a variety of diseases. *Saccharomyces cerevisiae* has served as a model to study mtDNA integrity, in part because it can survive without mtDNA. A measure of defective mtDNA in *S. cerevisiae* is the formation of *petite* colonies. The frequency at which spontaneous *petite* colonies arise varies by ~100-fold between laboratory and natural isolate strains. To determine the genetic basis of this difference, we applied quantitative trait locus (QTL) mapping to two strains at the opposite extremes of the phenotypic spectrum: the widely studied laboratory strain S288C and the vineyard isolate RM11-1a. Four main genetic determinants explained the phenotypic difference. Alleles of *SAL1*, *CAT5*, and *MIP1* contributed to the high *petite* frequency of S288C and its derivatives by increasing the formation of *petite* colonies. By contrast, the S288C allele of *MKT1* reduced the formation of *petite* colonies and compromised the growth of *petite* cells. The former three alleles were found in the EM93 strain, the founder that contributed ~88% of the S288C genome. Nearly all of the phenotypic difference between S288C and RM11-1a was reconstituted by introducing the common alleles of these four genes into the S288C background. In addition to the nuclear gene contribution, the source of the mtDNA influenced its stability. These results demonstrate that a few rare genetic variants with individually small effects can have a profound phenotypic effect in combination. Moreover, the polymorphisms identified in this study open new lines of investigation into mtDNA maintenance.

MITOCHONDRIA are responsible for many critical biological processes such as energy production via oxidative phosphorylation (Nelson and Cox 2000), intermediary metabolism (Nelson and Cox 2000), heme biosynthesis (Heinemann *et al.* 2008), iron–sulfur cluster biogenesis (Lill and Muhlenhoff 2008), the production of reactive oxygen (Balaban *et al.* 2005), and programmed cell death (Newmeyer and Ferguson-Miller 2003). Of the ~1000 gene products that function in the mitochondria, only a small subset are encoded in the mitochondrial genome (mtDNA) (Sickmann *et al.* 2003). This subset includes components of the mitochondrial protein translation apparatus and subunits of the protein complexes involved in oxidative phosphorylation (Taylor and Turnbull 2005).

In addition to energy production, oxidative phosphorylation generates the membrane potential ($\Delta\Psi$) across the inner membrane of the mitochondrion (Nelson and Cox 2000). $\Delta\Psi$ is required for the import of most nuclear-encoded proteins into the organelle (Mokranjac and Neupert 2008). Thus, mtDNA, which is essential for oxidative phosphorylation (Taylor and Turnbull 2005), is also important for the maintenance of $\Delta\Psi$. For this reason, mtDNA affects many of the biological processes that occur within the mitochondria.

Consistent with the importance of mtDNA integrity, many inherited mutations in mtDNA lead to a spectrum of human diseases that often affect multiple organ systems (Taylor and Turnbull 2005). In addition to inherited mtDNA mutations, acquired mtDNA mutations in somatic tissues accumulate progressively during the normal course of aging (Chomyn and Attardi 2003; Chien and Karsenty 2005). These somatic mtDNA mutations may play a causal role in age-associated diseases such as Parkinson's (Bender *et al.* 2006; Kraytsberg *et al.* 2006) and cancer (Ishikawa *et al.* 2008). Moreover, mice engineered with a proofreading-deficient mitochondrial DNA polymerase (Trifunovic *et al.* 2004) exhibit a premature aging phenotype that

Supporting information is available online at http://www.genetics.org/cgi/content/full/genetics.109.104497/DC1.

[1]*Corresponding author:* 1100 Fairview Ave. N., P.O. Box 19024, Seattle, WA 98109. E-mail: dgottsch@fhcrc.org

correlates with increased somatic mtDNA deletions (Vermulst *et al.* 2008).

The yeast *Saccharomyces cerevisiae* is an excellent model organism for gaining insights into the molecular basis of human mitochondrial disorders (Barrientos 2003). Unlike metazoans, *S. cerevisiae* is a facultative anaerobe and can survive without mtDNA, a situation that is not tolerated in obligate aerobes (Hance *et al.* 2005). Yeast cells with defective (*rho*$^-$) or no (*rho*^{0}) mitochondrial genome are referred to as *petite*s because they form small colonies on glucose-containing medium (Ephrussi *et al.* 1949; Dujon 1981). By contrast, cells that have fully functional mitochondria form *grande* colonies and are designated *rho*$^+$. Both *rho*$^-$ and *rho*^{0} cells can be propagated on a fermentable carbon source such as glucose, because they are able to generate ATP through glycolysis (Nelson and Cox 2000). However, they cannot grow on a nonfermentable carbon source such as glycerol, because under these conditions ATP synthesis can be achieved only through oxidative phosphorylation (Nelson and Cox 2000).

Mitochondrial genome instability can be quantitatively measured by the frequency of spontaneous *petites* in a population of yeast cells. While values can vary, the lowest *petite* frequencies are ~1% for *S. cerevisiae* (Sherman 2002). This low end of the spectrum is at least 100-fold higher than the expected occurrence of respiratory-defective yeast cells due to nuclear mutations (Tzagoloff and Dieckmann 1990; Drake 1991). Over 200 complementation groups of nuclear *S. cerevisiae* mutations leading to respiratory deficiency have been identified (Tzagoloff and Dieckmann 1990), and the spontaneous mutation rate per nuclear gene in *S. cerevisiae* ranges from 10^{-7} to 10^{-8} per cell division (Drake 1991). Given this mutation rate in nuclear genes, the spontaneous *petite* frequency generally reflects the instability of the mitochondrial rather than nuclear DNA (Dujon 1981).

More than 200 genes are required for the faithful maintenance of *rho*$^+$ yeast mtDNA (Contamine and Picard 2000; Hess *et al.* 2009). However, only a fraction of these genes are involved in pathways that directly affect mtDNA transactions such as replication, recombination, and repair, as well as mtDNA packaging into nucleoids, nucleoid division, and nucleoid segregation to daughter cells (Contamine and Picard 2000; Chen and Butow 2005). Loss-of-function mutations in these genes lead to *rho*$^-$ and/or *rho*^{0} *petite*s. The involvement of other processes—such as mitochondrial transcription and translation, ATP synthesis, iron homeostasis, and fatty acid metabolism—accounts for the majority of known loss-of-function mutations that increase *petite* production, but their involvement in mtDNA maintenance is not well understood (Contamine and Picard 2000).

The majority of spontaneously arising *petite* cells are *rho*$^-$ (de Zamaroczy *et al.* 1981). Analysis of the mtDNA in a number of spontaneous *petite* mutants suggests that most such *rho*$^-$ genomes are a head-to-tail tandem repetition of a segment of the *rho*$^+$ mtDNA (Faugeron-Fonty *et al.* 1979). The DNA sequence of the repeated segment in spontaneous *petite* mutants suggests that the repeat may originate from *rho*$^+$ mtDNA by illegitimate direct-repeat recombination involving short homologous sequences (Gaillard and Bernardi 1979; Gaillard *et al.* 1980). However, neither the defects in mtDNA processing that lead to direct-repeat recombination nor the conditions that may determine its occurrence are known.

Given the large number of genes that can modulate *petite* formation, it is not surprising that the spontaneous frequency of *petites* varies within a large range among laboratory strains of *S. cerevisiae* (Marmiroli *et al.* 1980; Sherman 2002). There have been two attempts in the past 50 years to explain the genetic basis for these differences. Soon after the discovery of the *petite* mutation (Ephrussi *et al.* 1949), Ephrussi's group identified a laboratory strain with very unstable mtDNA (Ephrussi and Hottinguer 1951). A single, recessive nuclear mutation was responsible for this phenotype, but the identity of the mutant gene was never determined. More recently, a single-nucleotide polymorphism (SNP) in the gene encoding the mitochondrial DNA polymerase (*MIP1*) was implicated in the increased mtDNA mutability of several common laboratory *S. cerevisiae* strains (Baruffini *et al.* 2007).

In the course of studying the age-associated genomic instability that occurs during yeast pedigree analysis (McMurray and Gottschling 2003), we discovered that *petite* formation can lead to increased nuclear genome instability (Veatch *et al.* 2009). To understand the basis for how mitochondrial defects arise, we sought to identify genetic determinants that were responsible for the spontaneous *petite* formation observed. We found that the frequency at which *petite*s arose in a culture varied among different strains of *S. cerevisiae*, which is consistent with earlier reports (Ephrussi and Hottinguer 1951; Marmiroli *et al.* 1980). In the study presented here, we use quantitative trait locus (QTL) mapping to identify the main genetic determinants of *petite* formation in the common laboratory strain S288C and its derivatives, which were used in our earlier nuclear genome instability studies (McMurray and Gottschling 2003; Veatch *et al.* 2009).

MATERIALS AND METHODS

Strains and plasmids: The segregants from the BY4716 (*MAT*α *lys2*Δ*0*) × RM11-1a (*MAT***a** *leu2*Δ*0 ura3*Δ*0 ho::loxP-kanMX4-loxP*) cross have been described in detail elsewhere (Brem *et al.* 2002; Yvert *et al.* 2003; Brem and Kruglyak 2005). A list of all the other strains used in this study can be found in Table 1. The construction of the allelic replacement strains is described in detail below. Isogenic haploid

TABLE 1

Yeast strains used in this study

Strain	Background	Relevant genotype	References or source
Σ1278b	Σ1278b	*MAT*α *SAL1 MKT1-30G CAT5-91M MIP1-661T*	F. Hilger (Gembloux)
EM93[a]	Progenitor of S288C	*MAT***a**/α *SAL1/sal1-1 MKT1-30G/MKT1-30G CAT5-91M/CAT5-91I MIP1-661T/MIP1-661A*	Mortimer and Johnston (1986)
UCC1158	RM11-1a	*MAT***a** *ho::loxP-KAN-loxP leu2*Δ*0 ura3*Δ*0 SAL1 MKT1-30G CAT5-91M MIP1-661T*	Mortimer *et al.* (1994)
BY4716	S288C	*MAT*α *lys2*Δ*0 sal1-1 MKT1-30D CAT5-91I MIP1-661A*	Brachmann *et al.* (1998)
S288C	S288C	*MAT*α *mal gal2 sal1-1 MKT1-30D CAT5-91I MIP1-661A*	Adams *et al.* (1997); Mortimer and Johnston (1986)
UCC1166	SK1	*MAT*α *ho::LYS2 leu2*Δ*(Asp18-EcoRI) lys2*Δ*0 ura3*Δ*0 SAL1 MKT1-30G CAT5-91M MIP1-661T*	Barbara Garvik (Hartwell Lab)
YDS3	W303	*MAT*α *ade2-1, trp1-1, can1-100, leu2-3,112, his3-11,15, ura3 RAP1 wt SAL1 MKT1-30G CAT5-91M MIP1-661A*	Lori Sussel (Shore Lab)
UCC8407	YPS163	*MAT***a** *ho::loxP-KANMX4-loxP SAL1 MKT1-30G CAT5-91M MIP1-661T*	This study
UCC8409	YPS1000	*MAT***a** *ho::loxP-KANMX4-loxP SAL1 MKT1-30G CAT5-91M MIP1-661T*	This study
UCC8411	YPS1009	*MAT***a** *ho::loxP-KANMX4-loxP SAL1 MKT1-30G CAT5-91M MIP1-661T*	This study
UCC8062-1	Diploid RM11	*MAT***a**/α *LEU2/leu2*Δ*0 LYS2/lys2*Δ*0 ura3*Δ*0/ura3*Δ*0 ho::loxP-KAN-loxP/ho::loxP-KAN-loxP*	This study
UCC8088-1	Diploidized BY4716	*MAT***a**/α *lys2*Δ*0/lys2*Δ*0*	This study
UCC8240	S288C	*MAT***a** *MKT1-30D ura3*Δ*0*	This study
UCC8241	S288C	*MAT***a** *MKT1-30G ura3*Δ*0*	This study
UCC8334	S288C	*MAT*α *lys2*Δ*0 [S288C rho*$^+$*]*	This study
UCC8335	S288C	*MAT*α *lys2*Δ*0 [S288C rho*$^+$*]*	This study
UCC8338	S288C	*MAT*α *lys2*Δ*0 [RM11 rho*$^+$*]*	This study
UCC8339	S288C	*MAT*α *lys2*Δ*0 [RM11 rho*$^+$*]*	This study
UCC8340	RM11	*MAT*α *ho::loxP-KAN-loxP lys2*Δ*0 ura3*Δ*0 [S288C rho*$^+$*]*	This study
UCC8341	RM11	*MAT*α *ho::loxP-KAN-loxP lys2*Δ*0 ura3*Δ*0 [S288C rho*$^+$*]*	This study
UCC8344	RM11	*MAT*α *ho::loxP-KAN-loxP lys2*Δ*0 ura3*Δ*0 [RM11 rho*$^+$*]*	This study
UCC8356	S288C	*MAT***a** *MKT1-30G sal1-1 CAT5-91I MIP1-661A ura3*Δ*0*	This study
UCC8357	S288C	*MAT***a** *MKT1-30G sal1-1 CAT5-91I MIP1-661T ura3*Δ*0*	This study
UCC8358	S288C	*MAT*α *MKT1-30G sal1-1 CAT5-91M MIP1-661A ura3*Δ*0*	This study
UCC8359	S288C	*MAT*α *MKT1-30G sal1-1 CAT5-91M MIP1-661T ura3*Δ*0*	This study
UCC8360	S288C	*MAT***a** *MKT1-30G SAL1 CAT5-91I MIP1-661A ura3*Δ*0*	This study
UCC8361	S288C	*MAT*α *MKT1-30G SAL1 CAT5-91I MIP1-661T ura3*Δ*0*	This study
UCC8362	S288C	*MAT***a** *MKT1-30G SAL1 CAT5-91M MIP1-661A ura3*Δ*0*	This study
UCC8363	S288C	*MAT*α *MKT1-30G SAL1 CAT5-91M MIP1-661T ura3*Δ*0*	This study
UCC8372	S288C	*MAT*α *MKT1-30G SAL1 CAT5-91M MIP1-661T ura3*Δ*0 [RM11 rho*$^+$*]*	This study
UCC8374	S288C	*MAT*α *MKT1-30G SAL1 CAT5-91M MIP1-661T ura3*Δ*0 [RM11 rho*$^+$*]*	This study
UCC8376	S288C	*MAT*α *MKT1-30G SAL1 CAT5-91M MIP1-661T ura3*Δ*0 [S288C rho*$^+$*]*	This study
UCC8378	S288C	*MAT*α *MKT1-30G SAL1 CAT5-91M MIP1-661T ura3*Δ*0 [S288C rho*$^+$*]*	This study
UCC8413	Hybrid BY4716 × RM11	*MAT***a**/α *LEU2/leu2*Δ*0 LYS2/lys2*Δ*0 URA3/ura3*Δ*0 ho/ho::loxP-kan-loxP*	This study

[a] A kind gift of Joshua Akey's lab.

derivatives of YPS163, YPS1000, and YPS1009 from Paul Sniegowski's collection of oak yeast isolates (Sniegowski *et al.* 2002) were created by inactivating the *HO* endonuclease with a *loxP-kanMX4-loxP* cassette (Guldener *et al.* 1996), sporulating the transformants, and selecting the haploid, G418 resistant spores. BY4716 was diploidized by using the pHS2 plasmid (a kind gift of Adam Deutschbauer) as previously described (Deutschbauer and Davis 2005).

The plasmid pLND44-4 was used to replace the *MIP1-661A* allele with the *MIP1-661T* allele. The plasmid pRS306-*MKT1*-D30G (a kind gift of Joshua Veatch) was used to replace the *MKT1-30D* allele with a *MKT1-30G* allele. Please refer

to supporting information, File S1, for details in plasmid construction.

Strain construction for functional analysis: The allelic exchange experiments were conducted in the BY4724 (*MAT***a** *lys2*Δ*0 ura3*Δ*0*) background to be able to use the *URA3* marker for positive and negative selection. The *MKT1* and *MIP1* allelic replacements were executed by a two-step gene replacement strategy using integrating, *URA3*-marked plasmids (Scherer and Davis 1979; Adams *et al.* 1997). For the *MKT1* replacement, we linearized pRS306-*MKT1*-D30G with *Hin*dIII before transformation. For the *MIP1* replacement, we linearized pLND44-4 with *Avr*II. In both cases, Ura$^+$ transformants were grown in YEPD to allow for the spontaneous excision of the integrated plasmid. These events were selected for by plating cells on 5-fluoroorotic acid (5-FOA) (Boeke *et al.* 1987). Several independent, 5-FOA resistant clones were sequenced to screen for those that had retained the new *MKT1-30G* or *MIP1-661T* alleles. The *SAL1* and *CAT5* allelic replacements were executed by two sequential transformations as described in detail elsewhere (Gray *et al.* 2004). Briefly, the first transformation integrates the *URA3* marker into the targeted locus (*sal1-1* or *CAT5-91I*). The second transformation replaces *URA3* with a PCR product, which in our case was amplified from RM11-1a genomic DNA (see File S1 for details).

In all single-allele replacement experiments, control replacements with the respective S288C/BY4716 (hereafter S288C/BY) alleles were performed in parallel to rule out background mutations during the transformation process that may reduce the *petite* frequency. Moreover, two independent transformants for each single replacement were analyzed and found to behave similarly. Proper allele replacements were sequence verified. PCR and sequencing primers are listed in Table S1.

The single-allelic replacement strains were all of the same mating type. After several crosses and sporulations, we constructed a diploid strain that is homozygous for *MKT1-30G* and heterozygous for *SAL1/sal1-1*, *CAT5-91M/CAT5-91I*, and *MIP1-661T/MIP1-661A*. All the strains in Figure 7 are haploid spores from that single diploid strain and thus isogenic for the S288C genetic background except at the indicated alleles for *SAL1*, *CAT5*, and *MIP1*.

Media and growth conditions: We used standard YEPD medium (1% yeast extract, 2% peptone, and 2% glucose). The indicator medium for the *petite* frequency assay was YEPDG (1% yeast extract, 2% peptone, 0.1% glucose, and 3% glycerol) (Adams *et al.* 1997). On this type of medium, respiratory-deficient cells give rise to much smaller colonies than respiratory-proficient cells (Tzagoloff and Dieckmann 1990). The difference in colony size between *petite*s and *grande*s is clearly distinguishable after growth at 30° for 5 days.

To compare the growth of *grande* cells (Figure 4C and Figure S1, A), we pregrew cells in YEPG (1% yeast extract, 2% peptone, and 3% glycerol) before plating serial dilutions on YEPD. A pure population of *petite* cells (Figure 4C, Figure S1, A and B) was derived by treating logarithmic-phase cells in YEPD with 25 μg/ml of ethidium bromide for 6 hr (Slonimski *et al.* 1968). After washing out the ethidium bromide, cells were either plated in serial dilutions on YEPD to compare the growth of *petite* cells or analyzed using a Powerwave XS plate reader (see File S1).

***Petite* frequency assay:** Strains were streaked onto YEPD plates from the glycerol freezer stock and allowed to grow into single colonies for 2 days. At least four independent colonies or independent groups of colonies were suspended in sterile 1× PBS. Appropriate PBS dilutions of each independent suspension were plated onto large YEPDG plates. The *petite* and *grande* colonies were counted after growth at 30° for 5 days. Colonies were counted manually for Figures 1B and 2 and with ImageJ 1.38x software (http://rsbweb.nih.gov/ij/) for Figures 1C, 4B, 7, and 8 (see File S1 for details). The reported *petite* frequency is the ratio of small colonies to total number of colonies. For each strain, we report the median *petite* frequency of the independent isolates to reduce the effects of any outliers due to jackpot events: *petite* mutations occurring very early during colony growth.

Linkage and statistical analysis: We tested for linkage between a marker and the *petite* frequency phenotype by dividing the segregants into two groups according to the inheritance of the BY or the RM11-1a (hereafter RM) marker allele. The median *petite* frequencies for the segregants in the BY *vs.* the RM group were compared with the nonparametric, Wilcoxon–Mann–Whitney test (Lindgren 1968). The *P*-value of that test was transformed by taking the negative value of the natural logarithm of the *P*-value to arrive at the "linkage likelihood" statistic reported in Figure 3. The 5% genomewide significance level in Figure 3 was estimated by empirical permutation tests (Churchill and Doerge 1994). Analogous results were obtained by running the linkage analysis in R/qtl (data not shown). The Wilcoxon–Mann–Whitney test was also used to assess the statistical significance of the difference in *petite* frequencies between two strains. Fisher's exact test (Prism software) was used to assess the statistical significance of the difference in *petite* mutation rates (Table 2).

Genome sequences and alignments: The source of the BY/S288C sequences was the Saccharomyces Genome Database (SGD) (http://www.yeastgenome.org/). The source of the RM11-1a sequences was the Broad Institute (http://www.broad.mit.edu/annotation/genome/*saccharomyces_cerevisiae*/). DNA or protein alignments between BY and RM were performed using the *blastn* and *blastp* functionalities respectively provided by the Broad Institute web site. For each gene in locus 2, protein alignments between BY and the other Saccharomyces genus species were performed on the SGD website by using the "Fungal Alignment" option in the "Comparison Resources" drop-down menu from the Summary SGD page for each gene. These alignments are generated by applying the ClustalW multiple sequence alignment algorithm to available sequences from the following six species: *S. paradoxus*, *S. mikatae*, *S. bayanus*, *S. kudriavzevii*, *S. castellii*, and *S. kluyveri* (Cliften *et al.* 2003; Kellis *et al.* 2003). Additional protein alignments between BY and species of the Ascomycetes phylum were performed on the SGD website by using the "BLASTP *vs.* fungi" option in the Comparison Resources drop-down menu from the Summary SGD page of the gene. The Ascomycetes species selected for these additional alignments were *Schizosaccharomyces pombe* (Wood *et al.* 2002), *Ashbya gossypii* (Dietrich *et al.* 2004), *Candida glabrata*, *Kluyveromyces lactis*, *Debaryomyces hansenii*, *Yarrowia lipolytica* (Dujon *et al.* 2004), and *Pichia stipitis* (Jeffries *et al.* 2007).

mtDNA swaps: *kar1*Δ*15* strains derived from BY4700 and RM11-1a served as donors for the BY and RM mitochondrial genomes. The *kar1*Δ*15* allele was introduced into these strains via a pop-in/pop-out strategy using plasmid pMR1593 (Vallen *et al.* 1992). The strains that served as recipients of the desired mtDNA were *rho*^{0} derivatives of BY4716 and RM11-1b. The *rho*^{0} strains were isolated by first transforming BY4716 and RM11-1b with pLND46, a derivative of p16G-*MIP1*-DN (kind gift of J. Veatch, unpublished data). pLND46 is a centromeric plasmid carrying the NatMX cassette as a selectable marker and a galactose-inducible, catalytically inactive allele of the mitochondrial DNA polymerase (*MIP1-D918A*). Transformants were induced to *rho*^{0} *petite*s by clonal growth on galactose and ClonNAT medium. These *rho*^{0} recipient strains and the *kar1*Δ*15* donor strains were mated for 4 hr at 30° on YEPD plates. Subsequently, individual zygotes

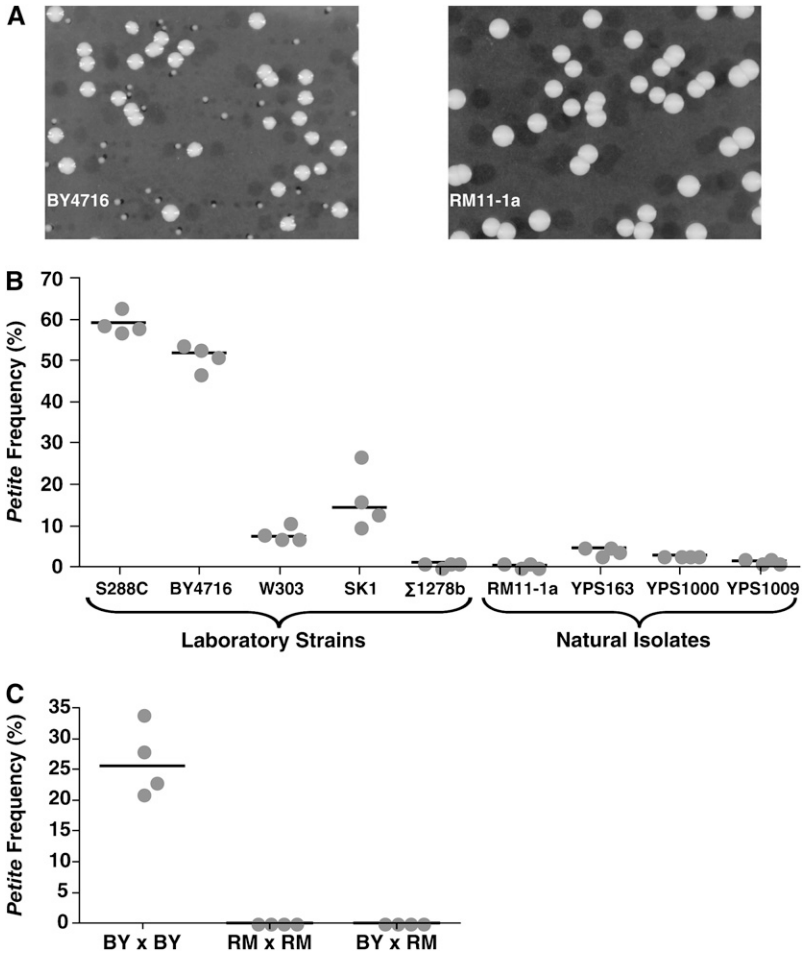

FIGURE 1.—*Petite*s occur at a higher frequency in most common laboratory strains. (A) A 2-day-old YEPD colony of the laboratory strain BY4716 and of the vineyard strain RM11-1a were diluted appropriately and plated onto indicator YEPDG plates to distinguish between *petite* and *grande* colonies. Pictures were taken after 5 days of growth. (B) *Petite* frequencies are presented for several laboratory and natural isolate strains (described in Tables 1 and 3). The *petite* frequency was determined for four independent isolates of each strain and is represented by a shaded dot. Each solid line represents the median *petite* frequency. (C) The *petite* frequencies for diploid strains of the BY (UCC8088-1), RM (UCC8062-1), and hybrid BY × RM (UCC8413) genetic backgrounds.

were micromanipulated to defined positions on the plate. Two hours later, individual vegetative cells were separated from the zygotes and placed at new positions on the plate. Colonies that arose from these vegetative cells were screened for the mating type and lysine auxotrophy of the recipient nuclear background. Transfer of the desired mitochondrial genome was confirmed by mtDNA isolation (described below) and *Eco*RV fingerprinting.

mtDNA isolation: Strains were grown in liquid YEPGal medium (1% yeast extract, 2% peptone, and 3% galactose). We find that strains with high mtDNA instability on glucose have robust mtDNA maintenance on galactose. Thus, growing the strains in galactose medium for mtDNA isolation allows us to obtain *grande* mtDNA genomes essentially unadulterated by *petite* genomes. The protocol follows the steps in DEFONTAINE *et al.* (1991) with the following modifications. We performed only two water washes before zymolyase treatment and did not sonicate after the lysis step. Cell debris and nuclei were pelleted at 4300 × *g* for 12 min. The supernatant was then pelleted at 20,000 × *g* for 20 min to obtain a crude mitochondrial pellet mostly devoid of contaminating nuclear DNA. RNAse A was added to the mitochondrial lysis buffer to a final concentration of 100 μg/ml. The DNA was phenol extracted and precipitated from the aqueous layer with 0.1 vol of sodium acetate and 1 vol of isopropanol. For the fingerprinting analysis, the isolated mtDNA was *Eco*RV digested and run on a 0.6% agarose gel overnight at 23 V.

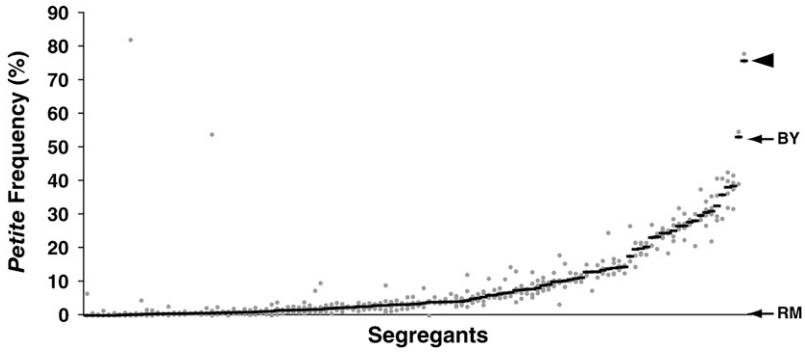

FIGURE 2.—*Petite* frequency is a quantitative trait. A total of 122 segregants from a cross between BY4716 and RM11-1a (BREM and KRUGLYAK 2005) were assayed for their *petite* frequencies. Each shaded dot represents the *petite* frequency of an independent isolate of a segregant. The solid dash indicates the median *petite* frequency for each segregant based on all independent isolates of that segregant. Segregants are sorted in increasing order of median *petite* frequency. The arrows point to the median *petite* frequencies of the parental strains (BY4716 at 52%, RM11-1a at 0.6%). The arrowhead points to the one segregant with median *petite* frequency greater than that of BY4716.

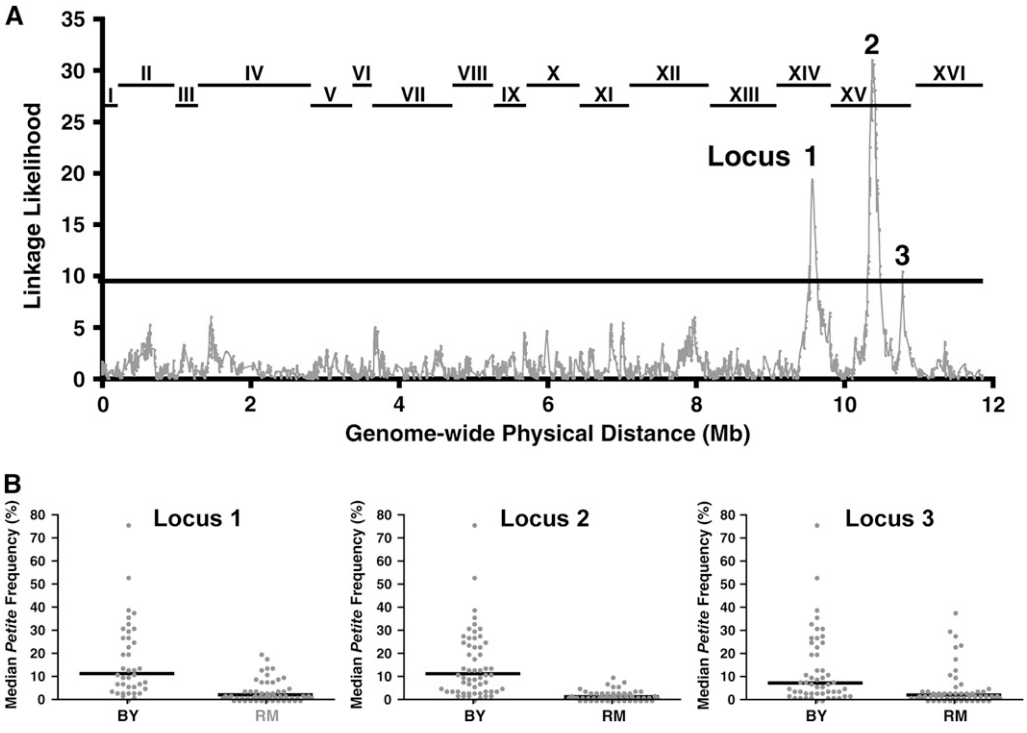

FIGURE 3.—The *petite* frequency phenotype links to at least 3 QTL. (A) Linkage between a polymorphic marker and the median *petite* frequency phenotype was tested by partitioning the segregants into two groups according to marker inheritance (BY or RM). The median *petite* frequencies were compared between the two groups with the Wilcoxon–Mann–Whitney statistical test (LINDGREN 1968). The *P*-value of that test was transformed by taking the negative value of the natural logarithm of the *P*-value. The shaded line plots the transformed *P*-value (*y*-axis) for each marker as a function of the physical location of the marker in the yeast genome (*x*-axis). The lines at the top of the graph indicate the locations of the 16 *S. cerevisiae* chromosomes. The solid line at linkage likelihood of 9.3 marks the 5% genomewide significance level, which is adjusted for multiple testing on the basis of empirical permutation tests (CHURCHILL and DOERGE 1994). The three loci that reach statistical significance are designated as loci 1, 2, and 3. (B) The median *petite* frequencies are presented for segregants with unequivocal inheritance at the three loci shown in A of either the BY or the RM parent. For locus 1, analysis was restricted to the 100 segregants with no missing genotype data and no recombination events in the 37.2-kbp window between marker positions 449,639 and 486,861, which are the two markers with the highest linkage likelihood. For locus 2, analysis was restricted similarly to 114 segregants in a 26.4-kbp window (between marker positions 519,776 and 546,197). For locus 3, analysis was similarly restricted to 108 segregants in an 8.7-kbp window between marker positions 937,036 and 945,781, which are the two markers with the highest linkage likelihood.

RESULTS

***Petites* occur at higher frequency in most common laboratory strains than in natural isolates:** To determine whether QTL mapping was a feasible method for identifying genetic determinants of *petite* formation, we took a representative set of *S. cerevisiae* strains and determined the frequency of *petite*s in these strains using a simple, quantitative measure. Briefly, colonies were grown for 2 days on rich medium with 2% glucose (YEPD), which does not require growing cells to have respiratory mitochondrial function. These colonies were then resuspended and plated onto rich medium with 0.1% glucose and 3% glycerol (YEPDG), on which colonies of *petite* cells are easily distinguished from colonies that arise from *grande* cells (Figure 1A) (ADAMS *et al.* 1997).

Using this assay, the *petite* frequencies of five commonly used laboratory strains and four natural *S. cerevisiae* isolates were measured (Figure 1B). The laboratory strains included S288C, which is a historical laboratory standard that was used as the source of the first completely sequenced eukaryotic genome (GOFFEAU *et al.* 1996). BY4716 is a direct descendant of S288C and served as the basis for the systematic deletion collection (WINZELER *et al.* 1999) and our earlier nuclear genome instability studies (MCMURRAY and GOTTSCHLING 2003; VEATCH *et al.* 2009). W303 is also derived in part from S288C, but its lineage appears to include crosses to several other unrelated strains (WINZELER *et al.* 2003; SCHACHERER *et al.* 2007). In contrast, Σ1278b and SK1 do not appear to have been derived from any crosses with S288C (LITI *et al.* 2009). The RM11-1a strain, a natural isolate from a California vineyard (MORTIMER *et al.* 1994), was chosen because of the QTL mapping resources available (BREM *et al.* 2002; YVERT *et al.* 2003). In addition, three natural isolates from oak trees were included because of their documented genetic diversity among wild *S. cerevisiae* populations (FAY and BENAVIDES 2005).

Petite frequencies were determined for haploid derivatives of all nine strains. All four natural *S. cerevisiae* isolates had low *petite* frequencies of <5% (Figure 1B). By contrast, four of the five laboratory strains had median *petite* frequencies that were higher than those of the natural isolates (Figure 1B). This disparity may indicate that extended propagation of *S. cerevisiae* strains in the laboratory reduces selection for high-fidelity maintenance of full mitochondrial genome

TABLE 2

Estimation of *petite* mutation rates per cell division

	Strain				
	UCC8240	UCC8241	UCC8360	UCC8358	UCC8357
Genotype					
MKT1	BY	RM	RM	RM	RM
SAL1	BY	BY	RM	BY	BY
CAT5	BY	BY	BY	RM	BY
MIP1	BY	BY	BY	BY	RM
Cell divisions					
Two *grandes*	56	38	54	55	55
Petite and *grande*	3	11	4	4	4
Petite mutation rate (%)	5	22	7	7	7
P-value		$<0.01^a$	0.03^b	0.03^b	0.03^b

[a] The test compares UCC8241 to UCC8240.

[b] The test compares UCC8360, 8358 or 8357 to UCC8241.

Cells were pregrown in liquid YEPG medium for at least 24 hr to select for a pure population of *grande* cells. An aliquot of the saturated YEPG culture (1:1000 dilution) was inoculated into YEPD medium. After 10 hr of growth in YEPD, individual unbudded or small-budded cells were picked as mothers and placed at predefined positions on a solid YEPD plate. Newly formed daughter cells were separated from their mother cells by micromanipulation, and the mother and daughter cells were allowed to form independent colonies. The *petite* and *grande* status of each cell was inferred from the phenotype of the resulting colony. For *MKT1*, BY indicates the *MKT1-30D* allele, and RM indicates the *MKT1-30G* allele. For *SAL1*, BY indicates the *sal1-1* allele, and RM indicates the wild-type allele. For *CAT5*, BY indicates the *CAT5-91I* allele, and RM indicates the *CAT5-91M* allele. For *MIP1*, BY indicates the *MIP1-661A* allele, and RM indicates the *MIP1-661T* allele.

function. More importantly, however, the results suggest that *petite* formation is a quantitative trait that could lend itself to QTL mapping.

***Petite* frequency is a quantitative trait in *S. cerevisiae*:** The high frequency of *petite* formation in BY4716 and low frequency in RM11-1a (Figure 1, A and B) provided a unique opportunity to identify the genetic determinants that were responsible for *petite* formation in BY4716 by QTL mapping. BY and RM were crossed and ~120 recombinant progeny from this cross were genotyped for parental contributions at 2957 polymorphic markers covering >99% of the yeast genome (Brem and Kruglyak 2005). These recombinants were used to map loci important in quantitative traits of gene expression (Brem *et al.* 2002; Yvert *et al.* 2003; Brem and Kruglyak 2005), stochastic variation in gene expression (Ansel *et al.* 2008), proteome variation (Foss *et al.* 2007), cell morphology (Nogami *et al.* 2007), and DNA repair sensitivity (Demogines *et al.* 2008) between BY and RM. Thus, it seemed likely that these same recombinants could be used to map relevant QTL that affected *petite* formation.

As a first step to determine if the difference in *petite* frequency between BY and RM had a genetic component, the *petite* frequency was determined for a diploid strain that was a cross between BY and RM. This hybrid exhibited a low *petite* frequency, similar to an RM × RM diploid strain, and very different from the relatively high *petite* frequency of a BY × BY strain (Figure 1C). These results suggested that the *petite* frequency phenotype was under genetic control and that the RM alleles were dominant to those in BY.

Next, 122 F_1 haploid segregants from the BY × RM cross were assayed for their median *petite* frequencies. These values formed a continuum (Figure 2), ranging from the value for the RM parent to the value for one segregant with a median *petite* frequency greater than that of the BY parent (Figure 2, arrowhead). These data indicated that the median *petite* frequency phenotype in the segregants was indeed a quantitative trait. Nineteen segregants had median *petite* frequencies that were at the same low level as that of the RM parent (<0.6%). If random segregation of unlinked loci and no epistasis are assumed, then these data suggested that at least three loci ($1/2^3 \approx 19/122$ F_1 segregants) were responsible for the low *petite* frequency of the RM parent. The influence of multiple loci on *petite* formation was also suggested by the presence of one segregant with a median *petite* frequency of 76% (Figure 2, arrowhead), which is higher than that of the BY parent (52%, Figure 1B). These data are consistent with transgressive segregation, in which nonparental allele combinations at more than one locus in the F_1 progeny produce a phenotype that is more extreme than either parental phenotype (Rieseberg *et al.* 2003).

Linkage analysis identifies three QTL for mtDNA instability: We tested for linkage between the inheritance of each of the available 2957 polymorphic markers and the median *petite* frequency phenotype (see materials and methods). Three QTL in the yeast genome

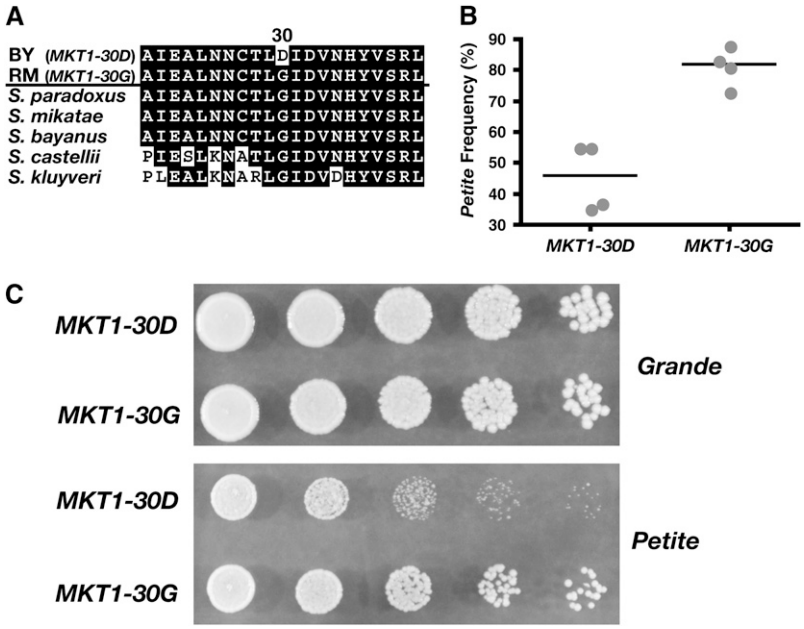

FIGURE 4.—*MKT1* is a QTG that affects the growth of *petite* cells. (A) Sequence alignment of the region of the Mkt1 protein that contains the nonsynonymous polymorphism at the 30th amino acid residue (indicated above the alignment). The most common amino acid at each position in the protein is boxed in black. (B) *Petite* frequencies of strains UCC8240 (*MKT1-30D*) and UCC8241 (*MKT1-30G*). (C) Serial dilution spotting of *grande* (top) and *petite* (bottom) cells of the strains UCC8240 (*MKT1-30D*) and UCC8241 (*MKT1-30G*). See MATERIALS AND METHODS for the isolation of pure populations of *grande* and *petite* cells.

reached statistical significance on the basis of permutation tests (Figure 3A) (CHURCHILL and DOERGE 1994). Locus 1 is on chromosome XIV. Loci 2 and 3 are both on chromosome XV but are likely to be unlinked genetically given the physical distance between them (~410 kbp). For all three QTL, inheritance of the RM alleles at each locus was associated with a lower *petite* frequency (Figure 3B).

***MKT1* is a quantitative trait gene that affects *petite* formation and the growth of *petite* cells:** Locus 1 coincides with QTL identified in other mapping studies in *S. cerevisiae*. A SNP in the *MKT1* gene contributes to the high-temperature-growth phenotypic difference between BY and a clinical isolate (STEINMETZ *et al.* 2002; SINHA *et al.* 2006), to the sporulation efficiency difference between BY and SK1 (DEUTSCHBAUER and DAVIS 2005), and to expression quantitative trait differences between BY and RM (ZHU *et al.* 2008). The *MKT1* allele that imparts high-temperature resistance (SINHA *et al.* 2006) and efficient sporulation (DEUTSCHBAUER and DAVIS 2005) encodes a glycine at the 30th amino acid (*MKT1-30G*) of the open reading frame (ORF). By contrast, the BY allele encodes an aspartate at residue 30 (*MKT1-30D* allele) (Figure 4A).

We next asked whether the same amino acid difference in *MKT1* affected the *petite* frequency phenotype. The *MKT1-30D* allele in the BY genetic background was replaced with an *MKT1-30G* allele (referred to as BY *MKT1-30G*) (see MATERIALS AND METHODS). The median *petite* frequency of the BY *MKT1-30G* strain was 82%, almost twice that of the BY *MKT1-30D* strain (Figure 4B). This result was unexpected because the linkage analysis predicted that inheritance of an RM allele at locus 1 was associated with a lower *petite* frequency (Figure 3B). These data indicated that another gene(s) within locus 1 contributed to the original QTL mapping information and provided a larger contribution to the RM-associated phenotype than did *MKT1-30G*.

The frequency at which *petite* cells arise in a population is a combination of two processes: the rate at which *petite* mutants are formed and their relative growth rate compared to the growth rate of *grande* cells in the population. We carried out single-cell analysis to measure the rate at which *petite* mutants were formed (Table 2). The *petite* mutation rate of the BY *MKT1-30D* strain was 5% while that of the BY *MKT1-30G* strain was 22% (Table 2), a difference that was statistically significant ($P = 0.01$). Thus, the *MKT1-30G* allele increases the rate of *petite* formation in the BY genetic background, a result consistent with this allele contributing to an increased *petite* frequency (Figure 4B).

Next, the growth rate of *grande* cells and newly derived *petite* cells was compared between the BY *MKT1-30D* and BY *MKT1-30G* strains. While there was no growth difference between the two strains when the cells were *grande*, the BY *MKT1-30G* strain exhibited a significant growth advantage over the BY *MKT1-30D* strain when the cells were *petite* (Figure 4C). Thus, two effects contributed to the higher *petite* frequency in BY *MKT1-30G* than in BY *MKT1-30D* cells. These were (1) a higher rate at which *petite* mutants were formed (Table 2) and (2) a growth advantage of the *petite* cells (Figure 4C) when the BY *MKT1-30G* strain was compared to the BY *MKT1-30D* strain.

The *MKT1-30D* allele is specific to the BY/S288C genetic background: The amino acid at residue 30 in Mkt1 occurs within a highly conserved region (Figure 4A) that is part of the nuclease domain of the protein (TADAUCHI *et al.* 2004). Mkt1 associates with Pbp1, which interacts with the Poly(A) binding protein near

TABLE 3

Strain genotypes at designated genes

	Laboratory strains					Natural isolates			
	S288C	BY4716	W303	SK1	Σ1278b	RM11-1a	YPS163	YPS1000	YPS1009
MKT1	BY	BY	RM	RM	RM	RM	RM	RM	RM
SAL1	BY	BY	RM	RM	RM	RM	RM	RM	RM
CAT5	BY	BY	RM	RM	RM	RM	RM	RM	RM
MIP1	BY	BY	BY	RM	RM	RM	RM	RM	RM

Genotypes of the laboratory and natural isolate strains from Figure 1B at the four QTGs are shown. The BY and RM alleles of each gene are described in the Table 2 legend.

the 3′ end of mRNAs (Tadauchi *et al.* 2004), and appears to regulate mRNA turnover via P bodies (Lee *et al.* 2009). However, the details of Mkt1 function are unclear. The glycine (*MKT1-30G*) allele in the RM strain is conserved at this position in all sequenced Saccharomyces species (Figure 4A). It is present in all the common laboratory strains and natural isolates we analyzed, except S288C and its derivative, BY4716 (Table 3). We also queried the Saccharomyces Genome Resequencing Project (SGRP) database (http://www.sanger.ac.uk/Teams/Team118/sgrp/ and Liti *et al.* 2009), which contains data on polymorphisms among S288C, W303, SK1, and 33 *S. cerevisiae* strains from diverse geographical regions and ecological niches. Sixteen of the 33 nonlaboratory *S. cerevisiae* isolates have high-quality sequence data for *MKT1*, and all of them carry the *MKT1-30G* allele. Thus, the *MKT1-30D* allele present in BY appears to be relatively rare and specific to the BY/S288C genetic background.

***SAL1*, *CAT5*, and *MIP1* are quantitative trait genes that affect *petite* formation:** We next wanted to determine which additional alleles within the three QTL contributed to the quantitative difference in *petite* frequency between the BY and RM strains. We had three considerations in developing our approach to identify these alleles. First, the hybrid BY × RM strain had a *petite* frequency similar to that of the RM × RM strain (Figure 1C), suggesting that the alleles in BY that contributed to its high *petite* frequency were recessive to the RM alleles. Second, the high *petite* frequency in BY/S288C strains was exceptional compared to that in the other strains examined (Figure 1B). Considering these two results together, we hypothesized that the recessive alleles in the BY strain represented partial or complete loss-of-function alleles in genes responsible for faithful mtDNA inheritance. These loss-of-function alleles were present in the BY strain and would be distinct from the normal functioning alleles of the same genes in the RM strain and other wild yeast isolates. Third, there is a polymorphism between BY and RM every ~1/200 nucleotides on average throughout the genome (Ronald *et al.* 2005). This divergence means that within the ~100-kbp region that defines locus 1 or locus 2, there are ~500 candidate polymorphisms that could explain the difference between the RM and BY *petite* frequencies.

With these ideas in mind, we took two parallel approaches to identify the relevant polymorphic differences within each locus. We examined candidate genes within the locus: those known to affect mitochondrial genome integrity or transmission (Contamine and Picard 2000). We also focused on nonsynonymous polymorphisms found within the coding region of genes at each locus. The latter approach meant that polymorphisms within intergenic regions (Tanay *et al.* 2005) or synonymous polymorphisms that might have a phenotypic effect (Kimchi-Sarfaty *et al.* 2007) were not considered. However, this approach provided an initial screening method to reduce the large number of possible candidates.

To look for polymorphisms, we used the whole-genome sequences available for the BY strain (SGD at http://yeastgenome.org/) and the RM11-1a strain (http://www.broad.mit.edu/annotation/genome/*saccharomyces_cerevisiae*/). A 100-kbp region around the peak linkage marker in locus 1 (Figure 5A) contained at least 294 polymorphisms between BY and RM (Figure 5A). A similar analysis in a 97-kbp region around the peak linkage marker in locus 2 (Figure 5B) identified at least 793 polymorphisms between BY and RM.

Locus 1: Within locus 1 (Figures 3A and 5A), the *SAL1* gene encodes a protein that appears to be a Ca^{2+}-dependent ATP-Mg/P_i exchanger in the mitochondrial inner membrane (Cavero *et al.* 2005; Traba *et al.* 2008). Loss-of-function mutations in *SAL1* result in decreased mtDNA transmission under certain growth conditions (Kucejova *et al.* 2008). *SAL1* contains a frameshift mutation (the *sal1-1* allele) in certain laboratory strains (Chen 2004). The locus history page in the SGD for *SAL1* documents that the *sal1-1* allele was corrected in the database in February 2004 after sequence comparisons to related fungi (Belenkiy *et al.* 2000; Brachat *et al.* 2003). We sequenced the *SAL1* gene from BY4716 and S288C. We discovered that these strains both contain the *sal1-1* allele despite the correction in the SGD (Figure 6A). The frameshift mutation results in the encoding of missense amino acids starting from the 403rd position of the protein onward (Figure 6B). The mutation also truncates the protein to 494 amino acids from its wild-type length of 545 amino acids. Thus, the

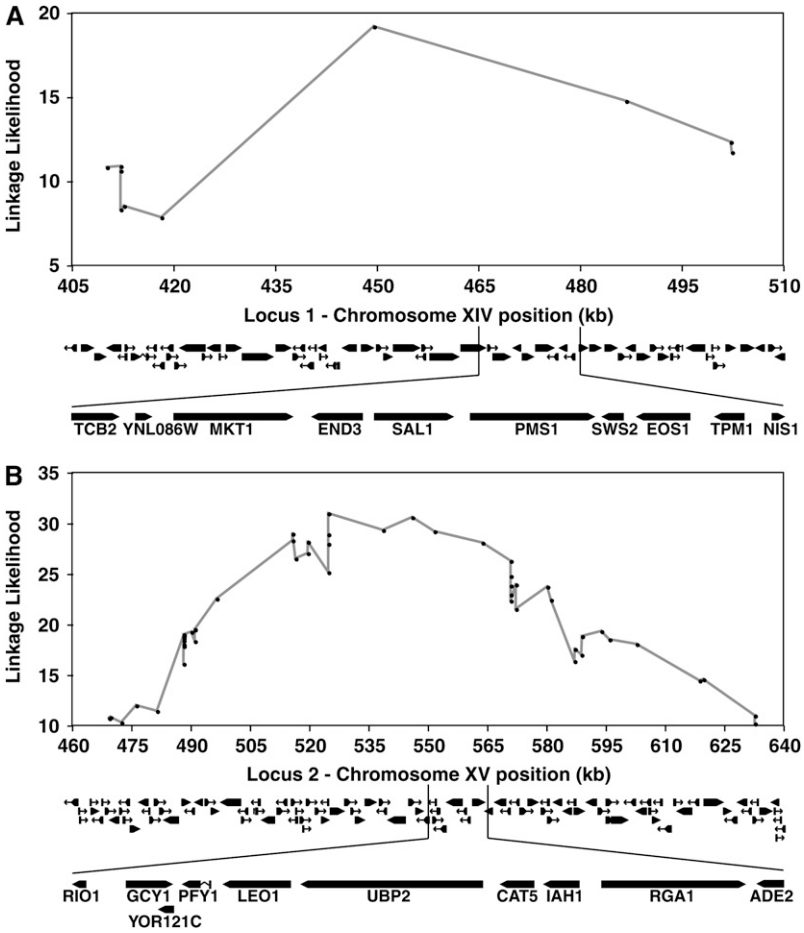

FIGURE 5.—Loci 1 and 2 contain a multitude of genes and polymorphisms that may cause the difference between the BY and RM *petite* frequencies. Graphical representations of the genes located in locus 1 (A) and locus 2 (B) are presented. The shaded lines plot the linkage likelihood for all the markers at each locus that reached the 5% genomewide statistical significance level (*y*-axis) as a function of physical location of the marker on chromosome XIV (A) and chromosome XV (B). Below the graphs are diagrams of all the protein-coding genes in these regions generated by the SGD GBrowse interface (www.yeastgenome.org). Below the diagrams are expansions of the subregions where QTGs implicated in this study were found: *MKT1* and *SAL1* (A) and *CAT5* (B). (A) The region between positions 410,121 and 510,213 was BLASTN aligned to the RM11-1a genome to reveal at least 294 polymorphisms between the two parental strains. (B) The region between positions 483,221 and 579,794 was BLASTN aligned to the RM11-1a genome to reveal at least 793 polymorphisms between the two parental strains (ALTSCHUL *et al.* 1997).

sal1-1 mutation is a good candidate for a partial or complete loss-of-function allele that potentially contributes to increased *petite* frequency in the BY genetic background (Figure 6, A and B).

To test the involvement of the *sal1-1* mutation in the *petite* frequency phenotype, we replaced the frameshift mutation in the BY background with the wild-type allele (see MATERIALS AND METHODS). The wild-type, RM allele of *SAL1*, in an otherwise BY *MKT1-30G* genetic background, suppressed the median *petite* frequency from 79% to 26% (Figure 7, compare columns 1 and 2). Thus, *SAL1* is a quantitative trait gene (QTG) that affects *petite* frequency.

Locus 2: In locus 2 (Figure 3A), we analyzed a 97-kbp region around the peak linkage marker (Figure 5B). In this region, there are a total of 47 genes and 109 nonsynonymous polymorphisms between the BY and RM strains. To reduce the number of possible polymorphisms to assay for *petite* frequency, we first considered only nonsynonymous polymorphisms between BY and RM in regions that were well conserved over the evolutionary timescale of Saccharomyces genus evolution [5–20 million years (KELLIS *et al.* 2003)]. Such polymorphisms are most likely to affect protein function (HANKS *et al.* 1988; CASARI *et al.* 1995). The ORFs of the 47 genes were aligned with the corresponding amino acid sequences from BY, RM, and six other sequenced species in the Saccharomyces genus (CLIFTEN *et al.* 2003; KELLIS *et al.* 2003). By requiring that the corresponding amino acid encoded in the RM strain be conserved, the number of polymorphism candidates was reduced from 109 to 8 (1 in *YVC1*, *RAS1*, *YOR114W*, *CAT5*, *RGA1*, and *ORT1* and 2 in *YOR093C*). An additional requirement for evolutionary conservation was placed by using sequences from seven more distantly related species of the Ascomycetes phylum, to which the Saccharomyces genus belongs (see MATERIALS AND METHODS). The estimated evolutionary distance between these additional Ascomycetes species is at least 300 million years (WOOD *et al.* 2002; DUJON *et al.* 2004). This additional constraint reduced the number of nonsynonymous polymorphisms for consideration from 8 to 2: one in the *CAT5* gene (Figure 6C) and the other in the *YOR114W* gene (Figure 6E).

CAT5 encodes a monooxygenase that localizes to mitochondria and catalyzes a step in the biosynthesis of ubiquinone, which is an electron carrier in the electron transport chain (ETC) (MARBOIS and CLARKE 1996; JONASSEN *et al.* 1998). The *CAT5* polymorphism gives rise to isoleucine in BY and methionine in RM at the 91st amino acid residue (Figure 6C). The BY isoleucine allele (*CAT5-91I*) was replaced with the RM

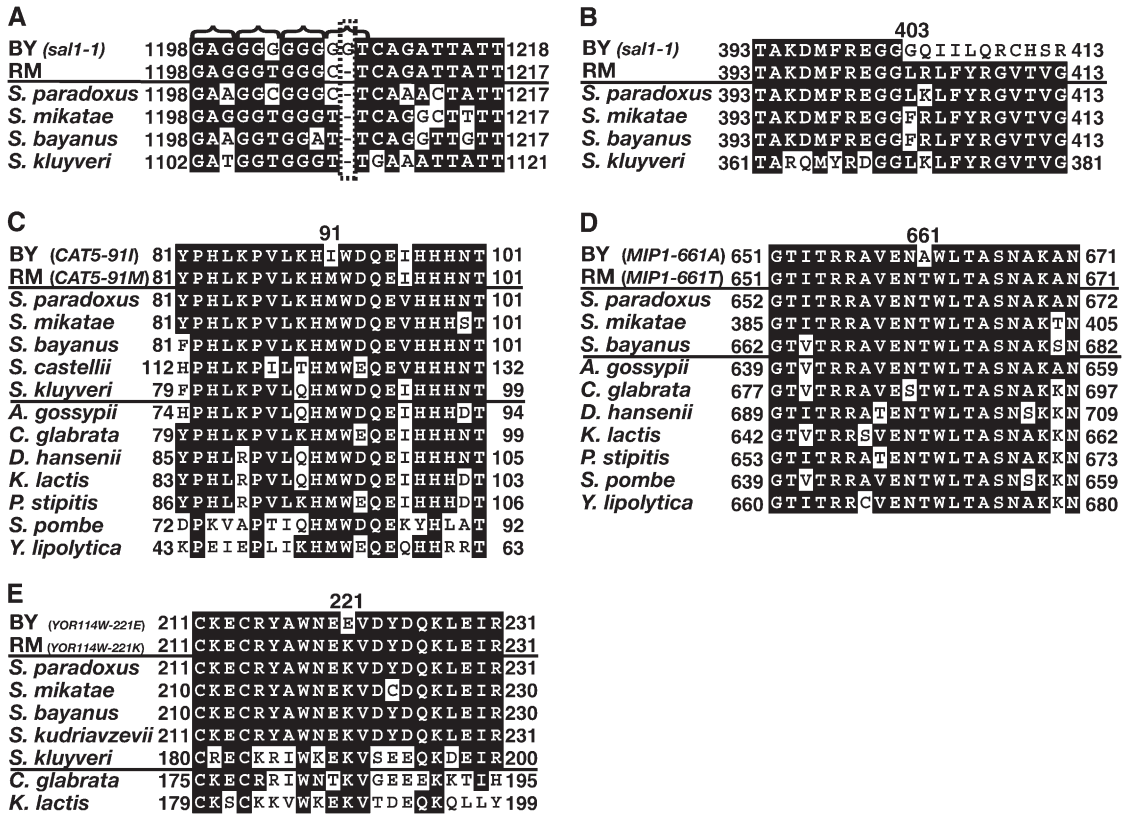

FIGURE 6.—The BY strain contains alleles of *SAL1*, *CAT5*, and *MIP1* that likely encode partial or complete loss-of-function proteins. (A) DNA sequence alignment of the region of the *SAL1* gene that contains the *sal1-1* allele in BY (the inserted nucleotide in the BY lineage is boxed with a dashed line). The brackets above the alignment indicate the register of the open reading frame. The *sal1-1* allele was also found in an old S288C isolate (not shown). The most common nucleotide at each position is boxed in black. (B) Sequence alignment of the Sal1 protein. The amino acid position of the frameshift is indicated above the alignment. Protein sequence alignments are shown of Cat5 (C), Mip1 (D), and YOR114W (E) from BY, RM, several closely related Saccharomyces species with available orthologs, and several distantly related Ascomycetes species with available orthologs. Only the regions of the sequence alignments that contain the relevant nonsynonymous polymorphisms are shown. RM contains the evolutionarily conserved ancestral allele while BY contains a derived allele. The position of the allele is numbered above the alignment. The most common amino acid within the Saccharomyces species at each position is boxed in black for all species.

methionine allele (*CAT5-91M*) (see MATERIALS AND METHODS). The *CAT5-91M* allele suppressed the median *petite* frequency from 79% in the BY *MKT1-30G CAT5-91I* strain to 51% in the BY *MKT1-30G CAT5-91M* strain (Figure 7, compare columns 1 and 3). Thus, *CAT5* is a QTG that affects the *petite* frequency phenotype. Allele replacement for the candidate polymorphism in *YOR114W* (Figure 6E), a gene of unknown function, did not affect the *petite* frequency phenotype (data not shown).

Locus 3: During the course of our study, an allele of *MIP1*, the mitochondrial DNA polymerase, was implicated in the elevated mtDNA mutability of some laboratory strains (BARUFFINI *et al.* 2007). This *MIP1* allele is present in BY, but not in RM. The polymorphism encodes alanine in BY and threonine in RM at the 661st amino acid of the Mip1 protein. The threonine at this position is conserved across the Saccharomyces and Ascomycetes species (Figure 6D). Thus, the BY allele was likely to encode a partial loss-of-function protein. These data, together with the fact that the allele was <2 kbp from the marker of peak linkage in locus 3 (Figure 3A), strongly implicated this polymorphism in *petite* formation. Therefore, the alanine allele (*MIP1-661A*) in BY was replaced with the RM threonine allele (*MIP1-661T*) at the *MIP1* genomic locus (see MATERIALS AND METHODS) and tested for *petite* frequency. The *MIP1-661T* allele suppressed the median *petite* frequency from 79% in the BY *MKT1-30G MIP1-661A* strain to 50% in the BY *MKT1-30G MIP1-661T* strain (Figure 7, compare columns 1 and 4). Thus, *MIP1* is a QTG that affects the *petite* frequency phenotype (BARUFFINI *et al.* 2007).

As previously mentioned, the *petite* frequency is a combination of the *petite* mutation rate and the relative growth rate of *petite* and *grande* cells. We measured the rate of *petite* formation in the different single-allele replacement strains (Table 2). We found that each one of the wild-type *SAL1*, *CAT5-91M*, or *MIP1-661T* alleles reduced the *petite* mutation rate in an otherwise BY *MKT1-30G* genetic background (Table 2). We also compared the growth of *grande* cells and of newly derived *petite* cells from the different allele replacement strains.

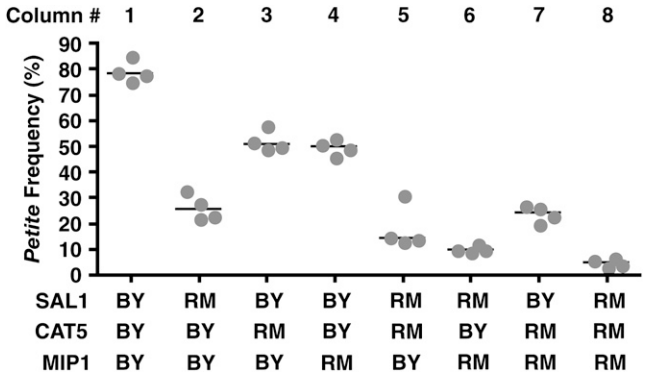

FIGURE 7.—*SAL1*, *CAT5*, and *MIP1* are QTGs that affect the *petite* frequency phenotype. *Petite* frequencies (as described in Figure 1) of strains containing each of the eight combinations of BY or RM alleles at the *SAL1*, *CAT5*, and *MIP1* QTGs are presented. All eight strains (UCC8356–UCC8363 in Table 1) are haploid spores derived from a single diploid BY strain that was homozygous for *MKT1-30G* and heterozygous for *SAL1/sal1-1*, *CAT5-91M/CAT5-91I*, and *MIP1-661T/MIP1-661A* (see MATERIALS AND METHODS). The BY and RM alleles of each gene are described in the Table 2 legend.

We did not see gross differences in the growth of *grande* or *petite* cells by the serial dilution assay (Figure S1, A). We also carried out a more detailed kinetic analysis of the growth of *petite* cells of the single-allele replacement strains (Figure S1, B). Under these more sensitive conditions, we observed a slight, but statistically significant, growth advantage for *petite* cells of the *CAT5-91M* and wild-type *SAL1* genotypes (Figure S1, B). Such an improvement in the growth of *petite* cells is expected to *increase* the *petite* frequency. However, the *CAT5-91M* and wild-type *SAL1* genotypes *decrease* the *petite* frequency (Figure 7, columns 2 and 3). Taken together, our results suggest that the *SAL1*, *CAT5*, and *MIP1* polymorphisms lower the *petite* frequency primarily by reducing the rate at which new *petite* cells are formed.

The *SAL1*, *CAT5*, and *MIP1* polymorphisms, in combination, account for nearly all the difference in *petite* formation between BY and RM: The difference in median *petite* frequency between BY and RM, when both contained the *MKT1-30G* allele, was >100-fold (79% for BY, Figure 7, *vs.* 0.6% for RM, Figure 1B). We next asked how much of this difference could be attributed to the *SAL1*, *CAT5*, and *MIP1* alleles and whether these alleles genetically interacted to contribute to this difference.

To address these questions, we created isogenic BY strains with all the possible combinations of BY or RM alleles in *SAL1*, *CAT5*, and *MIP1*. All eight strains had the *MKT1-30G* allele that gave robust growth of *petite* cells (Figure 4C). When all three BY alleles of *SAL1*, *CAT5*, and *MIP1* were present, the strain had a median *petite* frequency of 79% (Figure 7, column 1). In contrast, when all three RM alleles were present, the median *petite* frequency was 5% (Figure 7, column 8). As previously described, the median *petite* frequency of the original RM parental strain (also *MKT1-30G*) was 0.6% (Figure 1B). From these results, we conclude that the combination of the three polymorphisms in *SAL1*, *CAT5*, and *MIP1* explains ~94% [(79% − 5%)/(79% − 0.6%)] of the difference between the BY and RM strains when both carry the *MKT1-30G* allele.

Analysis of individual QTGs revealed that the *SAL1* allele had the greatest impact on *petite* frequency (Figure 7). When only the BY allele of *SAL1* was present, the strain had a median *petite* frequency of 24% (Figure 7, column 7). By contrast, individual BY alleles of *MIP1* and *CAT5* had median frequencies of 14 and 10%, respectively.

When pairs of alleles were combined, both additive and synergistic effects were obvious. The combination of *CAT5* and *MIP1* BY alleles appeared to have an additive affect on *petite* frequency; when both were present, the median *petite* frequency was 26% (Figure 7, column 2), compared with 10 and 14% individually. By contrast, when the BY allele of *SAL1* was combined with BY alleles of either *CAT5* or *MIP1*, there was evidence of nonadditive effects. Specifically, the median *petite* frequency of the strain with a single BY allele of *SAL1*, 24% (Figure 7, column 7), and of *CAT5*, 10% (Figure 7, column 6), added up to less than the median *petite* frequency of the strain with BY alleles of *SAL1* and *CAT5*, 50% (Figure 7, column 4). A similar, nonadditive interaction was observed for the combined effect of the *SAL1* and *MIP1* alleles (Figure 7, compare column 3 to the sum of columns 5 and 7). The most extreme deviation from an additive model was observed when all three loci were combined. The median *petite* frequency of the strain with a single BY allele of *SAL1*, 24% (Figure 7, column 7), of *CAT5*, 10% (Figure 7, column 6), and of *MIP1*, 14% (Figure 7, column 5), added up to less than two-thirds that of the triple BY allele strain, 79% (Figure 7, column 1).

The BY alleles of *SAL1*, *CAT5*, and *MIP1* are rare in natural isolates and originated in the main founder of the S288C strain: *Petite* formation in the BY/S288C strains was inordinately high compared to that in most other strains we examined (Figure 1B), and the high frequency resulted primarily from the alleles of *SAL1*, *CAT5*, and *MIP1* (Figure 7). Assuming *petite* formation does not provide a long-term benefit to the cell, we wondered how these three alleles came to be present in the BY/S288C strain background. We started by asking whether the *SAL1*, *CAT5*, and *MIP1* polymorphisms identified here were common or rare in *S. cerevisiae* strains. We sequenced these polymorphisms in the common laboratory strains and in the natural isolates that we analyzed for *petite* frequency (Figure 1B and Table 3). The BY/S288C alleles of *SAL1* and *CAT5* were not present in any of the other strains (Table 3). All these strains contained the RM alleles of these two genes. For *MIP1*, the BY allele was present in the W303 common laboratory strain, but the RM allele was present in the other six strains analyzed (Table 3). Extending

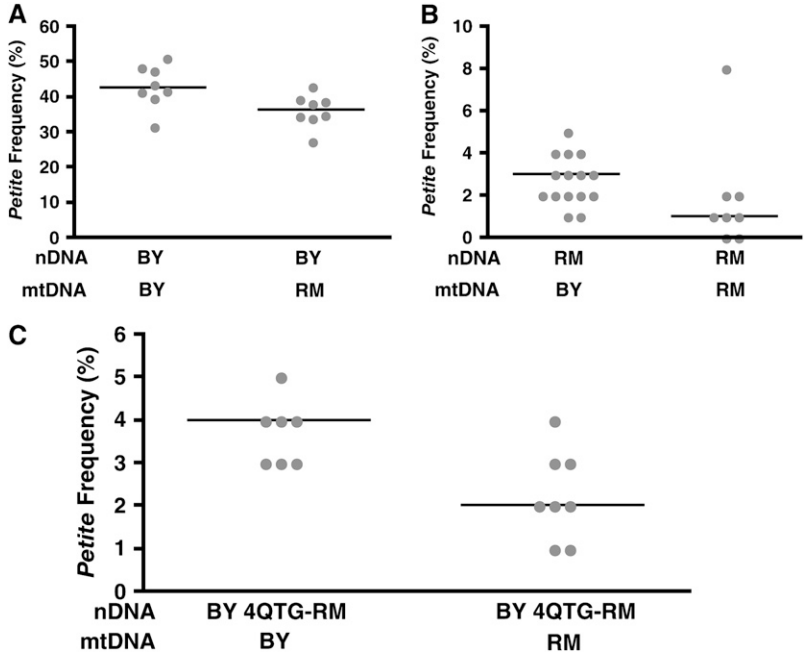

FIGURE 8.—The mitochondrial genome affects its own stability. *Petite* frequencies are shown of isonuclear strains with different mitochondrial genomes constructed via *kar* crosses (see MATERIALS AND METHODS). nDNA, nuclear DNA; mtDNA, mitochondrial DNA. (A) Pooled values from two independent isolates containing BY nDNA and BY mtDNA (UCC8334 and UCC8335) or BY nDNA and RM mtDNA (UCC8338 and UCC8339). (B) The same as in A except strains contain RM nDNA and BY mtDNA (UCC8340 and UCC8341) or RM nDNA and RM mtDNA (UCC8344). (C) BY or RM mtDNA was cytoduced by *kar* cross (see MATERIALS AND METHODS) into UCC8363, which is a BY background strain that contains the *MKT1-30G*, *SAL1*, *CAT5-91M*, and *MIP1-661T* alleles (referred to as BY 4QTG-RM). Shown are pooled values from two independent isolates containing BY 4QTG-RM nDNA and BY mtDNA (UCC8376 and UCC8378) or BY 4QTG-RM nDNA and RM mtDNA (UCC8372 and UCC8374).

this analysis to other natural isolates of *S. cerevisiae* revealed that the high-quality or imputed sequences of all 33 nonlaboratory strains in the SGRP database (http://www.sanger.ac.uk/Teams/Team118/sgrp/) contained the RM alleles of *SAL1*, *CAT5*, and *MIP1*. Thus, the BY alleles of these genes appear to be relatively rare in nature.

We next investigated the diploid EM93 strain, which is the main progenitor of S288C (MORTIMER and JOHNSTON 1986). We sequenced the four spores of an EM93 tetrad. We found that EM93 is heterozygous for *sal1-1* and contains both the *CAT5-91I* and *CAT5-91M* alleles, as well as both the *MIP1-661A* and *MIP1-661T* alleles (Figure S2). Thus, the BY alleles of *SAL1*, *CAT5*, and *MIP1*, which were all absent from the SGRP natural isolates, were all present in the EM93 diploid strain, but in a heterozygous state. We conclude that the most likely origin of the BY alleles of *SAL1*, *CAT5*, and *MIP1* is the EM93 strain, particularly given that this strain contributed ~88% of the S288C genome (MORTIMER and JOHNSTON 1986).

The mitochondrial genome affects its own stability: Our linkage analysis focused on nuclear genetic markers that were strongly associated with the *petite* frequency phenotype (Figure 3A). However, in addition to polymorphisms in the nuclear genome, variation in the mtDNA itself can affect *petite* frequency (CONTAMINE and PICARD 2000). As a first step to determine whether such a scenario affected the results reported here, the structure of the mitochondrial genome was analyzed in the BY and RM parent strains and in eight F_1 segregants (Figure 2). This set of eight segregants included those with the lowest (<1%) and highest (76%) median *petite* frequencies. *Eco*RV digestions of mtDNA isolated from each strain revealed restriction fragment length polymorphisms (RFLP) (BOTSTEIN *et al.* 1980) that differed between the BY and RM strains (Figure S3, compare lanes 2 and 3). In addition, the eight F_1 segregants were different from either parent, but all eight segregants were identical to one another. This latter result was consistent with the fact that all F_1 segregants were derived from a single BY4716 × RM11-1a hybrid, diploid clone (R. BREM, unpublished results). Moreover, the mtDNA restriction pattern of the eight F_1 segregants appeared to be a recombinant version of the two parental mitochondrial genomes. In *S. cerevisiae*, parental mtDNAs are free to recombine during zygote formation and homoplasmic, vegetative diploid cells are quickly established from the zygote (DUJON 1981). Thus, the diploid clone that was sporulated for the derivation of the F_1 segregants was homoplasmic for its mtDNA: a recombinant between the two parental mtDNAs. Given that eight F_1 segregants with a wide range of median *petite* frequencies all contained the same mtDNA, we conclude that the linkage analysis between *petite* frequency and nuclear genotype was not confounded by additional variation in the mtDNA segregating in the cross.

However, the question still remained whether the *petite* frequency, which differed so dramatically between the two haploid parents, was affected by the differences in the parental mitochondrial genomes. To address this question, isonuclear strains were created that contained the two different parental mitochondrial genomes (see MATERIALS AND METHODS). In BY isonuclear strains, an RM mtDNA resulted in a slight, but statistically significant, decrease in the median *petite* frequency when compared to BY mtDNA [from 43 to 36%, *P*-value = 0.02 (Figure 8A)]. Similarly, in RM isonuclear strains, RM

TABLE 4

Analysis of mitochondrial introns

Intron	Gene	PCR confirmation	
		BY	RM
aI1	*COX1*	+	–
aI5a	*COX1*	+	–
aI5b	*COX1*	+	–
aI5c	*COX1*	+	–
r1	*21S_rRNA*	+	–

Total DNA (nuclear and mitochondrial) from either the BY4716 or the RM11-1a strain was used as template in PCR reactions. Primer pairs (see Table S1) annealing to the exons that flank the listed introns were used. A minus (−) indicates that the PCR reaction amplified the shorter product, consistent with the absence of the respective intron in RM. A plus (+) indicates that the presence of the respective intron in BY was confirmed by PCR (see Table S1 for primers). Intron names are according to Pel and Grivell (1993).

mtDNA produced a slightly lower median *petite* frequency than BY mtDNA [from 3 to 1%, *P*-value <0.01 (Figure 8B)]. Finally, strains were created that contained the two different parental mtDNAs but had a common nuclear genetic background isogenic with BY except for the RM alleles at the four QTGs: *MKT1*, *SAL1*, *CAT5*, and *MIP1* (referred to here as BY 4QTG-RM). Even in a nuclear genetic background such as BY 4QTG-RM, which is associated with a very low *petite* frequency (Figure 7, column 8), the RM mtDNA led to an even lower median *petite* frequency than the BY mtDNA (Figure 8C). Thus, the RM mtDNA leads to a lower *petite* frequency regardless of the nuclear genetic background.

The result that the mitochondrial genome can affect its own stability suggested that either a polymorphic gene product or a *cis* feature of the RM mtDNA was responsible for its greater stability. One of the most common differences between yeast mitochondrial genomes is the presence or the absence of introns in the *COX1*, *COB*, and *21S_rRNA* genes (Dujon 1981; Pel and Grivell 1993). It is also known that intronless mtDNA is more stable than intron-containing mtDNA (Contamine and Picard 2000). To test whether such a situation may explain the difference in mtDNA stability between BY and RM, both mitochondrial genomes were examined for the presence of introns in the *COX1* and *21S_rRNA* genes (Table 4). The RM mtDNA genome lacked 5 of the 13 introns present in the BY mtDNA (Table 4). These structural variants between the BY and the RM mtDNA explain some of the differences in the *Eco*RV digestion pattern of the two mitochondrial genomes (Figure S3). Given that intronless mtDNA genomes are more stable (Contamine and Picard 2000), we speculate that the lack of some introns in the RM mtDNA causes its greater stability.

DISCUSSION

Taking advantage of QTL mapping methods, we have identified four alleles in the common budding yeast laboratory strains BY/S288C that account for nearly all of the difference in spontaneous *petite* frequency observed between these strains and natural isolates of *S. cerevisiae*. The BY/S288C alleles in the *SAL1*, *CAT5*, and *MIP1* genes combine to increase the *petite* frequency (Figure 7) primarily by increasing the rate of *petite* formation (Table 2). By contrast, the S288C-specific allele of *MKT1* reduces the *petite* frequency by lowering the rate of *petite* formation (Table 2) and by causing *petites* to grow very slowly and/or become inviable (Figure 4C). The identification of these alleles provides us with a genetic foundation for understanding how mitochondrial dysfunction can affect age-associated nuclear genome instability (McMurray and Gottschling 2003; Veatch *et al.* 2009). It also has practical implications for many yeast laboratories that use these strains, particularly those in which the presence of *petites* could affect the studies.

Origin of the BY/S288C alleles: The S288C variants of *MKT1*, *SAL1*, *CAT5*, and *MIP1* appear to be rare alleles when compared to the collection of 33 non-laboratory isolates of *S. cerevisiae* with sequenced genomes (Liti *et al.* 2009). However, we were able to trace the origin of the *sal1-1*, *CAT5-91I*, and *MIP1-661A* alleles in S288C to the EM93 strain, the main founder of the S288C strain (Mortimer and Johnston 1986). The fact that EM93 was isolated from a rotting fig in California raises the possibility that while rare, the S288C variants in *SAL1*, *CAT5*, and *MIP1* arose in the wild. Importantly, these rare variants are present in EM93 in the heterozygous state, complemented by the more common alleles. By contrast, EM93 is homozygous for the common *MKT1-30G* allele. Thus, the *MKT1-30D* allele in S288C is likely of laboratory origin.

We speculate that Mortimer inadvertently selected for the *MKT1-30D* allele during the creation of the S288C strain (Mortimer and Johnston 1986) because this allele reduces the *petite* frequency in the S288C genetic background (Figure 4B and Table 2). Moreover, the *MKT1-30D* allele produces a smoother colony morphology than the *MKT1-30G* allele (L. N. Dimitrov and D. E. Gottschling, unpublished observations). As we have shown here, the *MKT1-30G* allele permits *petite* cells to grow well, although they grow somewhat more slowly than *grande* cells (Figure 4C). When a cell with the *MKT1-30G* allele becomes *petite* during the growth of a colony, the cell and the somewhat slower growth of subsequent progeny produce a "lethal sector" or "nibbled" appearance in a colony (James and Werner 1966). By contrast, the *MKT1-30D* allele, which causes the *petite* cell to grow very slowly and/or die, cannot effectively compete against the growth of the *grande* cells

around it and hence does not contribute to the colony mass—there are no slow-growing sectors in the colony.

During the derivation of the S288C strain, Mortimer selected for strains that dispersed easily into single cells in liquid culture (Mortimer and Johnston 1986). One allele in S288C that contributes to easy dispersal is *flo8-1*, which contains a nonsense mutation that disrupts the function of the encoded transcription factor required for flocculation, diploid pseudohyphal growth, and haploid invasive growth (Liu *et al.* 1996). Another S288C allele that confers easy dispersal is *AMN1-368V* (Yvert *et al.* 2003; Ronald *et al.* 2005). However, the EM93 strain, which contributed 88% of its genome to S288C, contains a functional *FLO8* gene (Liu *et al.* 1996) and the more common *AMN1-368D* allele (Ronald and Akey 2007). Given the desire for cellular dispersal, it is easy to appreciate why the common EM93 alleles of *FLO8* and *AMN1* were not fixed in S288C. In contrast to *flo8-1* and *AMN1-368V*, the S288C alleles of *SAL1*, *CAT5*, and *MIP1* do not improve dispersal into single cells (data not shown). Nor are these alleles tightly linked to *FLO8* (or any of the other *FLO* genes) or to *AMN1*. Thus, it is unlikely that Mortimer selected for these alleles in deriving S288C from EM93. We favor the alternative possibility that these alleles randomly segregated into S288C during its derivation from EM93, a process in which several selection steps imposed severe genetic bottlenecks on the populations that eventually produced S288C (Mortimer and Johnston 1986). Due to this founder effect, the *sal1-1*, *CAT5-91I*, and *MIP1-661A* alleles are commonly encountered in laboratory strains (S288C and its derivatives). One reason why these alleles, which are mildly deleterious with respect to mtDNA inheritance, are still maintained in the S288C genetic background may be that the standards of care of laboratory strains do not place as strong a selective pressure on yeast populations as the selective pressure that occurs outside the laboratory environment (Figure 1B).

Comparison to other studies: Shortly after the discovery of *petite* colonies (Ephrussi *et al.* 1949), it was appreciated that the mtDNA in some yeast strains is unusually unstable (Ephrussi and Hottinguer 1951). For example, in one haploid strain from the Ephrussi lab (known as B_{15}), the *petite* mutation rate was found to be 4% per cell generation (Ephrussi and Hottinguer 1951). By crossing the B_{15} strain to one with a more stable mtDNA, the instability of the B_{15} strain was determined to be a recessive trait controlled by a single nuclear gene (Ephrussi and Hottinguer 1951). However, the identity of this gene was never determined. Our analysis of the *petite* mutation rate revealed that the mtDNA instability in BY was comparable to that of B_{15} (5% per cell generation; Table 2). The high mtDNA instability in BY was also a recessive trait. In contrast to Ephrussi's results, we found that the recessive trait was controlled by at least three nuclear QTL. By identifying a causative gene in each of these QTL, we have demonstrated the power of modern mapping technologies for dissecting ideas about unstable mtDNA phenotypes described >50 years ago.

Recently, a computation-based screen for genes that might affect mitochondrial function or transmission identified 100 single-deletion mutant alleles that significantly altered *petite* frequency relative to the wild-type BY/S288C strain that was used in the analysis (Hess *et al.* 2009). Interestingly, none of the *CAT5*, *MIP1*, *MKT1*, and *SAL1* genes was identified in this screen. Of these four genes, only *MIP1* (the gene encoding the mitochondrial DNA polymerase) is present in the compendium of nuclear-encoded genes that have been examined for altered *petite* frequency since the original Ephrussi work (Contamine and Picard 2000). Our results demonstrate that QTL mapping provides a complementary approach for understanding the complexity of mitochondrial genome maintenance and transmission.

The *MIP1-661A* allele was recently implicated as the cause for the mtDNA instability observed in most laboratory strains (Baruffini *et al.* 2007). Consistent with this study, we found that replacing the *MIP1-661A* allele at its genomic locus with the *MIP1-661T* allele partially suppressed the *petite* frequency phenotype (Figure 7). However, our analysis identified at least two other polymorphisms, namely those in *SAL1* and *CAT5*, that contributed to the increased mtDNA instability of S288C-derived laboratory strains (Figure 7). This difference is most easily explained by the fact that the prior study used a W303-derived strain for the allele swapping and phenotypic analysis. In W303, the *MIP1* allele is the only one that is derived from S288C, while the *CAT5*, *MKT1*, and *SAL1* alleles are the same as the common alleles in RM11-1a and the natural isolates (Table 3).

From a QTL mapping point of view, there are at least three studies that used *S. cerevisiae* as a model system to dissect the genetic architecture of a quantitative trait down to the molecular level (Steinmetz *et al.* 2002; Deutschbauer and Davis 2005; Gerke *et al.* 2009). Each one of these studies implicated three QTGs in their quantitative phenotypes: high temperature growth or sporulation efficiency. Our study reveals a comparable complexity in the genetic architecture of a quantitative trait by identifying four QTGs in three QTL. Moreover, the success in dissecting the *petite* frequency phenotype with 120 segregants demonstrates that it is possible to identify the main genetic determinants of a quantitative trait despite genetic interactions among the QTGs.

Mechanism of spontaneous *petite* formation: The prevailing model for the mechanism of spontaneous *petite* formation in *S. cerevisiae* postulates that *petite* genomes arise from the wild-type mtDNA by illegitimate direct-repeat recombination, which is facilitated by the

high prevalence of repetitive DNA in the mitochondrial genome (Bernardi 2005). Since Mip1, the mitochondrial DNA polymerase, is directly involved in replicating the mtDNA, we speculate that the S288C *MIP1-661A* allele leads to defects in mtDNA replication that increase the likelihood of illegitimate direct-repeat recombination. In yeast nuclear DNA, it has been shown that reduced expression of the replicative DNA polymerase α leads to increased homologous recombination events between yeast retrotransposons (Ty elements) on separate yeast chromosomes (Lemoine *et al.* 2005). The preferred sites for DNA double-strand breaks, which initiate recombination, involve two Ty elements that are in close proximity and have the potential to form a hairpin-like secondary structure (Lemoine *et al.* 2005). The mitochondrial genome of *S. cerevisiae* contains several putative origin-of-replication (*ori*) sequences that could also form hairpin-like secondary structures (de Zamaroczy *et al.* 1981). By analogy to Ty-mediated recombination, we propose that the *MIP1-661A* allele reduces the abundance of the Mip1 protein, leads to slow-moving replication forks, or gives rise to other perturbations in mtDNA replication that expose the *ori* sequences as fragile sites of double-strand DNA. Illegitimate recombination with *ori* sequences elsewhere in the mtDNA can lead to the production of *petite* genomes that are a subset of the rho^+ mtDNA. Consistent with this model, the vast majority of spontaneous *petite* genomes contain an mtDNA *ori* sequence (de Zamaroczy *et al.* 1981).

We hypothesize that unlike the direct effect of *MIP1* on mtDNA maintenance, *SAL1* and *CAT5* act indirectly by affecting the maintenance of an electrical potential across the inner mitochondrial membrane ($\Delta\Psi$). $\Delta\Psi$ is critical for the normal maintenance of mtDNA (Chen 2002; Wang *et al.* 2008). This gradient is required for import of nuclear-encoded mitochondrial proteins, including those involved in mitochondrial genome replication and maintenance (Mokranjac and Neupert 2008). Two ways that yeast cells grown on glucose, as was done in this study, can generate $\Delta\Psi$ are (1) through the ETC, which pumps protons across the inner membrane into the intermembrane space (Nelson and Cox 2000), and (2) through ATP synthase, which normally uses the proton gradient to make ATP, but can "run backward" whereby it hydrolyzes ATP located in the matrix to generate a proton gradient (Traba *et al.* 2008). This latter process is coupled with mitochondrial ATP transporters, which provide a source of ATP inside the matrix (Dupont *et al.* 1985; Smith and Thorsness 2008). Thus, when yeast are grown on glucose, their mitochondria consume, rather than produce, ATP (Traba *et al.* 2008).

SAL1 encodes a mitochondrial ATP carrier that transports ATP into the mitochondrial matrix through the mitochondrial inner membrane (Cavero *et al.* 2005). Thus, the ATP imported into the matrix by Sal1 fuels the maintenance of $\Delta\Psi$. We propose that the *sal1-1* allele reduces the efficiency of this transport and compromises the ability of the mitochondria to maintain a robust $\Delta\Psi$. Cat5 is a monooxygenase required for the biosynthesis of ubiquinone, a critical component of the ETC (Marbois and Clarke 1996; Jonassen *et al.* 1998). Here again, we propose that the *CAT5-91I* allele compromises the maintenance of $\Delta\Psi$ on glucose. Together, the *sal1-1* and *CAT5-91I* alleles affect mtDNA maintenance indirectly; they both compromise $\Delta\Psi$.

Considerations for mapping complex polygenic traits: Mitochondrial genome instability is, to various degrees, a common phenotype in *S. cerevisiae* laboratory strains (Figure 1B). As noted above, it is affected by a plethora of genes (Contamine and Picard 2000; Hess *et al.* 2009). We have identified alleles in three such genes (*SAL1*, *CAT5*, and *MIP1*) that in combination produce a high mtDNA instability in the BY/S288C strain. These three alleles account for nearly all of the phenotypic difference between BY and RM (Figure 7). However, these alleles cannot fully explain the phenotype of the extreme F_1 segregant with 76% median *petite* frequency (Figure 2, arrowhead). On the basis of our allele interaction analysis (Figure 7), we expected the genotype of this segregant to be *MKT1-30G*, *sal1-1*, *CAT5-91I*, and *MIP1-661A*. We sequenced this segregant at the four QTGs and found that its genotype deviated from our expectation at the *MKT1* gene; *i.e.*, it was *MKT1-30D* rather than *MKT1-30G* (data not shown). Thus, additional loci affecting *petite* frequency must be segregating in the BY × RM cross to result in an extreme phenotype that cannot be fully explained by the four QTGs. We did not detect statistically significant linkage to additional genomic loci presumably because their individual effect on *petite* frequency was too small. However, we propose that these additional loci, in combination, can contribute to the high mtDNA instability observed in the extreme F_1 segregant (Figure 2, arrowhead). Similar epistatic interactions that are hard to detect by conventional genetic crosses have been uncovered by using whole-chromosome substitutions in mammals (Shao *et al.* 2008).

While the three polymorphisms in *SAL1*, *CAT5*, and *MIP1* account for nearly all the phenotypic difference between BY and RM, in another laboratory strain, SK1, the high mtDNA instability is not due to any of the S288C-specific variants (Figure 1B and Table 3). Thus, more than one genetic architecture can give rise to a complex phenotype such as *petite* frequency, which is affected by multiple genes (Contamine and Picard 2000; Hess *et al.* 2009). The difference between SK1 and BY/S288C and the presence of the extreme F_1 segregant (Figure 2, arrowhead) are sobering reminders of the concept of *genotypic equivalence*: different combinations of alleles can confer effectively the same phenotype (Weiss 2008). Genotypic equivalence predicts that determining all the alleles in the human population that contribute to the emergence of polygenic human

disease phenotypes will be quite challenging given the large number of genes that can affect complex phenotypes (Weiss 2008). Thus, current efforts in human genetics such as whole-genome association studies (McCarthy *et al.* 2008) and resequencing of candidate genes for rare variants (Cohen *et al.* 2004; Ji *et al.* 2008) are probably uncovering only the tip of the genotypic iceberg.

We thank current and former members of the Gottschling laboratory for critical reading of this manuscript and many helpful discussions during the course of this study. We thank Michael McMurray for making the original observation of low *petite* frequency in RM11-1a, Erin Smith for providing valuable insights into the allelic replacements of candidate genes, Joshua Bloom for running the linkage analysis in R/qtl, Joshua Akey for the EM93 strain and help with the SGRP database, Joshua Veatch for the pRS306-*MKT1*-D30G and p16G-*MIP1*-DN plasmids, Adam Deutschbauer for the pHS2 plasmid, Paul Sniegowski for the wild oak yeast isolates, Kin Chan for suggesting the idea of scanning plates for colony counting, and David McDonald of the Fred Hutchinson Cancer Research Center Scientific Imaging Shared Resources for help with ImageJ. This work was supported by a Simon Fellowship from the Department of Genome Sciences, University of Washington (to L.N.D.), by a Burroughs-Wellcome Career Award at the Scientific Interface (to R.B.B.), by National Institutes of Health (NIH) grant R37 MH059520 and a James S. McDonnell Foundation Centennial Fellowship (to L.K.), and by NIH grant R01 AG023779 (to D.E.G.).

LITERATURE CITED

Adams, A., D. E. Gottschling, C. A. Kaiser and T. Stearns, 1997 *Methods in Yeast Genetics*. Cold Spring Harbor Laboratory Press, Cold Spring Harbor, NY.

Altschul, S. F., T. L. Madden, A. A. Schaffer, J. Zhang, Z. Zhang *et al.*, 1997 Gapped BLAST and PSI-BLAST: a new generation of protein database search programs. Nucleic Acids Res. **25:** 3389–3402.

Ansel, J., H. Bottin, C. Rodriguez-Beltran, C. Damon, M. Nagarajan *et al.*, 2008 Cell-to-cell stochastic variation in gene expression is a complex genetic trait. PLoS Genet. **4:** e1000049.

Balaban, R. S., S. Nemoto and T. Finkel, 2005 Mitochondria, oxidants, and aging. Cell **120:** 483–495.

Barrientos, A., 2003 Yeast models of human mitochondrial diseases. IUBMB Life **55:** 83–95.

Baruffini, E., T. Lodi, C. Dallabona and F. Foury, 2007 A single nucleotide polymorphism in the DNA polymerase gamma gene of *Saccharomyces cerevisiae* laboratory strains is responsible for increased mitochondrial DNA mutability. Genetics. **177:** 1227–1231.

Belenkiy, R., A. Haefele, M. B. Eisen and H. Wohlrab, 2000 The yeast mitochondrial transport proteins: new sequences and consensus residues, lack of direct relation between consensus residues and transmembrane helices, expression patterns of the transport protein genes, and protein-protein interactions with other proteins. Biochim. Biophys. Acta **1467:** 207–218.

Bender, A., K. J. Krishnan, C. M. Morris, G. A. Taylor, A. K. Reeve *et al.*, 2006 High levels of mitochondrial DNA deletions in substantia nigra neurons in aging and Parkinson disease. Nat. Genet. **38:** 515–517.

Bernardi, G., 2005 Lessons from a small, dispensable genome: the mitochondrial genome of yeast. Gene **354:** 189–200.

Boeke, J. D., J. Trueheart, G. Natsoulis and G. R. Fink, 1987 5-Fluoroorotic acid as a selective agent in yeast molecular genetics. Methods Enzymol. **154:** 164–175.

Botstein, D., R. L. White, M. Skolnick and R. W. Davis, 1980 Construction of a genetic linkage map in man using restriction fragment length polymorphisms. Am. J. Hum. Genet. **32:** 314–331.

Brachat, S., F. S. Dietrich, S. Voegeli, Z. Zhang, L. Stuart *et al.*, 2003 Reinvestigation of the *Saccharomyces cerevisiae* genome annotation by comparison to the genome of a related fungus: Ashbya gossypii. Genome Biol. **4:** R45.

Brachmann, C. B., A. Davies, G. J. Cost, E. Caputo, J. Li *et al.*, 1998 Designer deletion strains derived from *Saccharomyces cerevisiae* S288C: a useful set of strains and plasmids for PCR-mediated gene disruption and other applications. Yeast **14:** 115–132.

Brem, R. B., and L. Kruglyak, 2005 The landscape of genetic complexity across 5,700 gene expression traits in yeast. Proc. Natl. Acad. Sci. USA **102:** 1572–1577.

Brem, R. B., G. Yvert, R. Clinton and L. Kruglyak, 2002 Genetic dissection of transcriptional regulation in budding yeast. Science **296:** 752–755.

Casari, G., C. Sander and A. Valencia, 1995 A method to predict functional residues in proteins. Nat. Struct. Biol. **2:** 171–178.

Cavero, S., J. Traba, A. Del Arco and J. Satrustegui, 2005 The calcium-dependent ATP-Mg/Pi mitochondrial carrier is a target of glucose-induced calcium signalling in *Saccharomyces cerevisiae*. Biochem. J. **392:** 537–544.

Chen, X. J., 2002 Induction of an unregulated channel by mutations in adenine nucleotide translocase suggests an explanation for human ophthalmoplegia. Hum. Mol. Genet. **11:** 1835–1843.

Chen, X. J., 2004 Sal1p, a calcium-dependent carrier protein that suppresses an essential cellular function associated with the Aac2 isoform of ADP/ATP translocase in *Saccharomyces cerevisiae*. Genetics. **167:** 607–617.

Chen, X. J., and R. A. Butow, 2005 The organization and inheritance of the mitochondrial genome. Nat. Rev. Genet. **6:** 815–825.

Chien, K. R., and G. Karsenty, 2005 Longevity and lineages: toward the integrative biology of degenerative diseases in heart, muscle, and bone. Cell **120:** 533–544.

Chomyn, A., and G. Attardi, 2003 MtDNA mutations in aging and apoptosis. Biochem. Biophys. Res. Commun. **304:** 519–529.

Churchill, G. A., and R. W. Doerge, 1994 Empirical threshold values for quantitative trait mapping. Genetics **138:** 963–971.

Cliften, P., P. Sudarsanam, A. Desikan, L. Fulton, B. Fulton *et al.*, 2003 Finding functional features in *Saccharomyces* genomes by phylogenetic footprinting. Science. **301:** 71–76.

Cohen, J. C., R. S. Kiss, A. Pertsemlidis, Y. L. Marcel, R. McPherson *et al.*, 2004 Multiple rare alleles contribute to low plasma levels of HDL cholesterol. Science **305:** 869–872.

Contamine, V., and M. Picard, 2000 Maintenance and integrity of the mitochondrial genome: a plethora of nuclear genes in the budding yeast. Microbiol. Mol. Biol. Rev. **64:** 281–315.

Defontaine, A., F. M. Lecocq and J. N. Hallet, 1991 A rapid miniprep method for the preparation of yeast mitochondrial DNA. Nucleic Acids Res. **19:** 185.

Demogines, A., E. Smith, L. Kruglyak and E. Alani, 2008 Identification and dissection of a complex DNA repair sensitivity phenotype in Baker's yeast. PLoS Genet. **4:** e1000123.

Deutschbauer, A. M., and R. W. Davis, 2005 Quantitative trait loci mapped to single-nucleotide resolution in yeast. Nat. Genet. **37:** 1333–1340.

de Zamaroczy, M., R. Marotta, G. Faugeron-Fonty, R. Goursot, M. Mangin *et al.*, 1981 The origins of replication of the yeast mitochondrial genome and the phenomenon of suppressivity. Nature. **292:** 75–78.

Dietrich, F. S., S. Voegeli, S. Brachat, A. Lerch, K. Gates *et al.*, 2004 The Ashbya gossypii genome as a tool for mapping the ancient *Saccharomyces cerevisiae* genome. Science **304:** 304–307.

Drake, J. W., 1991 A constant rate of spontaneous mutation in DNA-based microbes. Proc. Natl. Acad. Sci. USA **88:** 7160–7164.

Dujon, B., 1981 Mitochondrial genetics and function, pp. 505–635 in *The Molecular Biology of the Yeast Saccharomyces: Life Cycle and Inheritance*, edited by J. N. Strathern, E. W. Jones and J. R. Broach. Cold Spring Harbor Laboratory Press, Cold Spring Harbor, NY.

Dujon, B., D. Sherman, G. Fischer, P. Durrens, S. Casaregola *et al.*, 2004 Genome evolution in yeasts. Nature **430:** 35–44.

Dupont, C. H., J. P. Mazat and B. Guerin, 1985 The role of adenine nucleotide translocation in the energization of the inner membrane of mitochondria isolated from rho + and rho degree

strains of *Saccharomyces cerevisiae*. Biochem. Biophys. Res. Commun. **132:** 1116–1123.

Ephrussi, B., and H. Hottinguer, 1951 On an unstable cell state in yeast. Cold Spring Harbor Symp. Quant. Biol. **16:** 75–85.

Ephrussi, B., H. Hottinguer and Y. Chimenes, 1949 Action de l'acriflavine sur les levures. I. La mutation "petite colonie.". Ann. Inst. Pasteur **76:** 351–367.

Faugeron-Fonty, G., F. Culard, G. Baldacci, R. Goursot, A. Prunell *et al.*, 1979 The mitochondrial genome of wild-type yeast cells. VIII. The spontaneous cytoplasmic "petite" mutation. J. Mol. Biol. **134:** 493–537.

Fay, J. C., and J. A. Benavides, 2005 Evidence for domesticated and wild populations of *Saccharomyces cerevisiae*. PLoS Genet. **1:** 66–71.

Foss, E. J., D. Radulovic, S. A. Shaffer, D. M. Ruderfer, A. Bedalov *et al.*, 2007 Genetic basis of proteome variation in yeast. Nat. Genet. **39:** 1369–1375.

Gaillard, C., and G. Bernardi, 1979 The nucleotide sequence of the mitochondrial genome of a spontaneous "petite" mutant of yeast. Mol. Gen. Genet. **174:** 335–337.

Gaillard, C., F. Strauss and G. Bernardi, 1980 Excision sequences in the mitochondrial genome of yeast. Nature **283:** 218–220.

Gerke, J., K. Lorenz and B. Cohen, 2009 Genetic interactions between transcription factors cause natural variation in yeast. Science **323:** 498–501.

Goffeau, A., B. G. Barrell, H. Bussey, R. W. Davis, B. Dujon *et al.*, 1996 Life with 6000 genes. Science **274**(546): 563–567.

Gray, M., M. Kupiec and S. M. Honigberg, 2004 Site-specific genomic (SSG) and random domain-localized (RDL) mutagenesis in yeast. BMC Biotechnol. **4:** 7.

Guldener, U., S. Heck, T. Fielder, J. Beinhauer and J. H. Hegemann, 1996 A new efficient gene disruption cassette for repeated use in budding yeast. Nucleic Acids Res. **24:** 2519–2524.

Hance, N., M. I. Ekstrand and A. Trifunovic, 2005 Mitochondrial DNA polymerase gamma is essential for mammalian embryogenesis. Hum. Mol. Genet. **14:** 1775–1783.

Hanks, S. K., A. M. Quinn and T. Hunter, 1988 The protein kinase family: conserved features and deduced phylogeny of the catalytic domains. Science **241:** 42–52.

Heinemann, I. U., M. Jahn and D. Jahn, 2008 The biochemistry of heme biosynthesis. Arch. Biochem. Biophys. **474:** 238–251.

Hess, D. C., C. L. Myers, C. Huttenhower, M. A. Hibbs, A. P. Hayes *et al.*, 2009 Computationally driven, quantitative experiments discover genes required for mitochondrial biogenesis. PLoS Genet. **5:** e1000407.

Ishikawa, K., K. Takenaga, M. Akimoto, N. Koshikawa, A. Yamaguchi *et al.*, 2008 ROS-generating mitochondrial DNA mutations can regulate tumor cell metastasis. Science **320:** 661–664.

James, A. P., and M. M. Werner, 1966 Radiation-induced lethal sectoring in yeast. Radiat. Res. **29:** 523–536.

Jeffries, T. W., I. V. Grigoriev, J. Grimwood, J. M. Laplaza, A. Aerts *et al.*, 2007 Genome sequence of the lignocellulose-bioconverting and xylose-fermenting yeast Pichia stipitis. Nat. Biotechnol. **25:** 319–326.

Ji, W., J. N. Foo, B. J. O'Roak, H. Zhao, M. G. Larson *et al.*, 2008 Rare independent mutations in renal salt handling genes contribute to blood pressure variation. Nat. Genet. **40:** 592–599.

Jonassen, T., M. Proft, F. Randez-Gil, J. R. Schultz, B. N. Marbois *et al.*, 1998 Yeast Clk-1 homologue (Coq7/Cat5) is a mitochondrial protein in coenzyme Q synthesis. J. Biol. Chem. **273:** 3351–3357.

Kellis, M., N. Patterson, M. Endrizzi, B. Birren and E. S. Lander, 2003 Sequencing and comparison of yeast species to identify genes and regulatory elements. Nature **423:** 241–254.

Kimchi-Sarfaty, C., J. M. Oh, I. W. Kim, Z. E. Sauna, A. M. Calcagno *et al.*, 2007 A "silent" polymorphism in the MDR1 gene changes substrate specificity. Science **315:** 525–528.

Kraytsberg, Y., E. Kudryavtseva, A. C. McKee, C. Geula, N. W. Kowall *et al.*, 2006 Mitochondrial DNA deletions are abundant and cause functional impairment in aged human substantia nigra neurons. Nat. Genet. **38:** 518–520.

Kucejova, B., L. Li, X. Wang, S. Giannattasio and X. J. Chen, 2008 Pleiotropic effects of the yeast Sal1 and Aac2 carriers on mitochondrial function via an activity distinct from adenine nucleotide transport. Mol. Genet. Genomics **280:** 25–39.

Lee, S. I., A. M. Dudley, D. Drubin, P. A. Silver, N. J. Krogan *et al.*, 2009 Learning a prior on regulatory potential from eQTL data. PLoS Genet. **5:** e1000358.

Lemoine, F. J., N. P. Degtyareva, K. Lobachev and T. D. Petes, 2005 Chromosomal translocations in yeast induced by low levels of DNA polymerase a model for chromosome fragile sites. Cell **120:** 587–598.

Lill, R., and U. Muhlenhoff, 2008 Maturation of iron-sulfur proteins in eukaryotes: mechanisms, connected processes, and diseases. Annu. Rev. Biochem. **77:** 669–700.

Lindgren, B. W., 1968 *Statistical Theory*. Macmillan, New York.

Liti, G., D. M. Carter, A. M. Moses, J. Warringer, L. Parts *et al.*, 2009 Population genomics of domestic and wild yeasts. Nature **458:** 337–341.

Liu, H., C. A. Styles and G. R. Fink, 1996 *Saccharomyces cerevisiae* S288C has a mutation in FLO8, a gene required for filamentous growth. Genetics **144:** 967–978.

Marbois, B. N., and C. F. Clarke, 1996 The COQ7 gene encodes a protein in *Saccharomyces cerevisiae* necessary for ubiquinone biosynthesis. J. Biol. Chem. **271:** 2995–3004.

Marmiroli, N., F. M. Restivo, C. Donnini, L. Bianchi and P. P. Puglisi, 1980 Analysis of rho mutability in *Saccharomyces cerevisiae*. I. Effects of mmc and pet-ts alleles. Mol. Gen. Genet. **177:** 581–588.

McCarthy, M. I., G. R. Abecasis, L. R. Cardon, D. B. Goldstein, J. Little *et al.*, 2008 Genome-wide association studies for complex traits: consensus, uncertainty and challenges. Nat. Rev. Genet. **9:** 356–369.

McMurray, M. A., and D. E. Gottschling, 2003 An age-induced switch to a hyper-recombinational state. Science **301:** 1908–1911.

Mokranjac, D., and W. Neupert, 2008 Energetics of protein translocation into mitochondria. Biochim. Biophys. Acta **1777:** 758–762.

Mortimer, R. K., and J. R. Johnston, 1986 Genealogy of principal strains of the yeast genetic stock center. Genetics **113:** 35–43.

Mortimer, R. K., P. Romano, G. Suzzi and M. Polsinelli, 1994 Genome renewal: a new phenomenon revealed from a genetic study of 43 strains of *Saccharomyces cerevisiae* derived from natural fermentation of grape musts. Yeast **10:** 1543–1552.

Nelson, D. L., and M. M. Cox, 2000 *Lehninger Principles of Biochemistry*. W. H. Freeman, San Francisco.

Newmeyer, D. D., and S. Ferguson-Miller, 2003 Mitochondria: releasing power for life and unleashing the machineries of death. Cell **112:** 481–490.

Nogami, S., Y. Ohya and G. Yvert, 2007 Genetic complexity and quantitative trait loci mapping of yeast morphological traits. PLoS Genet. **3:** e31.

Pel, H. J., and L. A. Grivell, 1993 The biology of yeast mitochondrial introns. Mol. Biol. Rep. **18:** 1–13.

Rieseberg, L. H., A. Widmer, A. M. Arntz and J. M. Burke, 2003 The genetic architecture necessary for transgressive segregation is common in both natural and domesticated populations. Philos. Trans. R. Soc. Lond. B Biol. Sci. **358:** 1141–1147.

Ronald, J., and J. M. Akey, 2007 The evolution of gene expression QTL in *Saccharomyces cerevisiae*. PLoS ONE **2:** e678.

Ronald, J., R. B. Brem, J. Whittle and L. Kruglyak, 2005 Local regulatory variation in *Saccharomyces cerevisiae*. PLoS Genet. **1:** e25.

Schacherer, J., D. M. Ruderfer, D. Gresham, K. Dolinski, D. Botstein *et al.*, 2007 Genome-wide analysis of nucleotide-level variation in commonly used *Saccharomyces cerevisiae* strains. PLoS ONE **2:** e322.

Scherer, S., and R. W. Davis, 1979 Replacement of chromosome segments with altered DNA sequences constructed in vitro. Proc. Natl. Acad. Sci. USA **76:** 4951–4955.

Shao, H., L. C. Burrage, D. S. Sinasac, A. E. Hill, S. R. Ernest *et al.*, 2008 Genetic architecture of complex traits: large phenotypic effects and pervasive epistasis. Proc. Natl. Acad. Sci. USA **105:** 19910–19914.

Sherman, F., 2002 Getting started with yeast. Methods Enzymol. **350:** 3–41.

Sickmann, A., J. Reinders, Y. Wagner, C. Joppich, R. Zahedi *et al.*, 2003 The proteome of *Saccharomyces cerevisiae* mitochondria. Proc. Natl. Acad. Sci. USA **100:** 13207–13212.

Sinha, H., B. P. Nicholson, L. M. Steinmetz and J. H. McCusker, 2006 Complex genetic interactions in a quantitative trait locus. PLoS Genet. **2:** e13.

Slonimski, P. P., G. Perrodin and J. H. Croft, 1968 Ethidium bromide induced mutation of yeast mitochondria: complete transformation of cells into respiratory deficient non-chromosomal "petites". Biochem. Biophys. Res. Commun. **30:** 232–239.

Smith, C. P., and P. E. Thorsness, 2008 The molecular basis for relative physiological functionality of the ADP/ATP carrier isoforms in *Saccharomyces cerevisiae*. Genetics **179:** 1285–1299.

Sniegowski, P. D., P. G. Dombrowski and E. Fingerman, 2002 *Saccharomyces cerevisiae* and *Saccharomyces paradoxus* coexist in a natural woodland site in North America and display different levels of reproductive isolation from European conspecifics. FEMS Yeast Res. **1:** 299–306.

Steinmetz, L. M., H. Sinha, D. R. Richards, J. I. Spiegelman, P. J. Oefner *et al.*, 2002 Dissecting the architecture of a quantitative trait locus in yeast. Nature **416:** 326–330.

Tadauchi, T., T. Inada, K. Matsumoto and K. Irie, 2004 Posttranscriptional regulation of HO expression by the Mkt1-Pbp1 complex. Mol. Cell. Biol. **24:** 3670–3681.

Tanay, A., A. Regev and R. Shamir, 2005 Conservation and evolvability in regulatory networks: the evolution of ribosomal regulation in yeast. Proc. Natl. Acad. Sci. USA **102:** 7203–7208.

Taylor, R. W., and D. M. Turnbull, 2005 Mitochondrial DNA mutations in human disease. Nat. Rev. Genet. **6:** 389–402.

Traba, J., E. M. Froschauer, G. Wiesenberger, J. Satrustegui and A. Del Arco, 2008 Yeast mitochondria import ATP through the calcium-dependent ATP-Mg/Pi carrier Sal1p, and are ATP consumers during aerobic growth in glucose. Mol. Microbiol. **69:** 570–585.

Trifunovic, A., A. Wredenberg, M. Falkenberg, J. N. Spelbrink, A. T. Rovio *et al.*, 2004 Premature ageing in mice expressing defective mitochondrial DNA polymerase. Nature **429:** 417–423.

Tzagoloff, A., and C. L. Dieckmann, 1990 PET genes of *Saccharomyces cerevisiae*. Microbiol. Rev. **54:** 211–225.

Vallen, E. A., M. A. Hiller, T. Y. Scherson and M. D. Rose, 1992 Separate domains of KAR1 mediate distinct functions in mitosis and nuclear fusion. J. Cell Biol. **117:** 1277–1287.

Veatch, J. R., M. A. McMurray, Z. W. Nelson and D. E. Gottschling, 2009 Mitochondrial dysfunction leads to nuclear genome instability: a link through iron-sulfur clusters. Cell **137:** 1247–1258.

Vermulst, M., J. Wanagat, G. C. Kujoth, J. H. Bielas, P. S. Rabinovitch *et al.*, 2008 DNA deletions and clonal mutations drive premature aging in mitochondrial mutator mice. Nat. Genet. **40:** 392–394.

Wang, X., K. Salinas, X. Zuo, B. Kucejova and X. J. Chen, 2008 Dominant membrane uncoupling by mutant adenine nucleotide translocase in mitochondrial diseases. Hum. Mol. Genet. **17:** 4036–4044.

Weiss, K. M., 2008 Tilting at quixotic trait loci (QTL): an evolutionary perspective on genetic causation. Genetics **179:** 1741–1756.

Winzeler, E. A., D. D. Shoemaker, A. Astromoff, H. Liang, K. Anderson *et al.*, 1999 Functional characterization of the *S. cerevisiae* genome by gene deletion and parallel analysis. Science **285:** 901–906.

Winzeler, E. A., C. I. Castillo-Davis, G. Oshiro, D. Liang, D. R. Richards *et al.*, 2003 Genetic diversity in yeast assessed with whole-genome oligonucleotide arrays. Genetics **163:** 79–89.

Wood, V., R. Gwilliam, M. A. Rajandream, M. Lyne, R. Lyne *et al.*, 2002 The genome sequence of *Schizosaccharomyces pombe*. Nature **415:** 871–880.

Yvert, G., R. B. Brem, J. Whittle, J. M. Akey, E. Foss *et al.*, 2003 Trans-acting regulatory variation in *Saccharomyces cerevisiae* and the role of transcription factors. Nat. Genet. **35:** 57–64.

Zhu, J., B. Zhang, E. N. Smith, B. Drees, R. B. Brem *et al.*, 2008 Integrating large-scale functional genomic data to dissect the complexity of yeast regulatory networks. Nat. Genet. **40:** 854–861.

Communicating editor: P. C. Phillips

GENETICS

Supporting Information
http://www.genetics.org/cgi/content/full/genetics.109.104497/DC1

Polymorphisms in Multiple Genes Contribute to the Spontaneous Mitochondrial Genome Instability of *Saccharomyces cerevisiae* S288C Strains

Lazar N. Dimitrov, Rachel B. Brem, Leonid Kruglyak and Daniel E. Gottschling

DOI: 10.1534/genetics.109.104497

FILE S1

Supporting Materials & Methods

Plasmid construction details: pLND44-4 was created by cloning into pRS306 (SIKORSKI and HIETER 1989) a fusion PCR product amplified from the mix of a left and a right PCR reaction as templates. The left PCR reaction used primers XhoI_*MIP1*_F (GTCTCG*CTCGAG*CCCGTAATATGGTCGAAGGA) and *MIP1*_661Thr_R (AACCACG**t**ATTTTCCACAGCTCTTCTAGTGATT), and S288C genomic DNA as template. The right PCR reaction used primers *MIP1*_661Thr_F (AATCACTAGAAGAGCTGTGGAAAAT**a**CGTGGTT) and EagI_SCD5_R (CGAGAC*CGGCCG*GATGGCCTCTTTTCTGCTTG), and S288C genomic DNA as template. The fusion PCR product was digested with *Xho*I and *Eag*I (italicized and underlined in XhoI_*MIP1*_F and EagI_SCD5_R) and was ligated into similarly digested pRS306. The *MIP1*_661Thr_R and *MIP1*_661Thr_F primers are responsible for introducing one nucleotide difference (bold lower case) from the S288C genome. This change replaces the GCG codon for alanine at the 661st position of *MIP1* in S288C with a threonine codon (**a**CG in the *MIP1*_661Thr_F primer). Sequence verification of pLND44-4 revealed that the cloned insert contains one additional nucleotide change 987 base pairs downstream of the intended single nucleotide change at the 661st amino acid of *MIP1*. This mutation was most likely introduced by the PCR amplification. During the pop-in/pop-out strategy for *MIP1* allele replacement with pLND44-4, we made sure that the pop-out recombination excised this secondary mutation out of the genomic DNA.

pRS306-*MKT1*-D30G was also created by cloning into pRS306 a fusion PCR product. The left PCR reaction used primers mkt1-1-SpeI (GATC*ACTAGT*ACCACCAAAACAGCTCATCAA) and mkt1-D30G-1 (CATAATGGTTGACGTCTATAcC**t**AGGGTACAATTATTCAG), and S288C genomic DNA as template. The right PCR reaction used primers mkt1-D30G-2 (CTGAATAATTGTACCCTaG**g**TATAGACGTCAACCATTATG) and mkt1-2-XhoI (GATC*CTCGAG*ATCAAACAGCTGAGGAACTGGA), and S288C genomic DNA as template. The fusion PCR product was digested with *Spe*I and *Xho*I (italicized and underlined) and was ligated into similarly digested pRS306. The mkt1-D30G-1 and mkt1-D30G-2 primers are responsible for introducing two nucleotide differences (lower case letters) from the S288C genome. One nucleotide change (bold lower case) changes the G**A**T codon for aspartate at the 30th amino acid position of *MKT1* in S288C into a glycine codon (G**g**T in the mkt1-D30G-2 primer). The other nucleotide change (non-bold lower case) changes the wobble position of the CTG codon for leucine at the 29th amino acid position of *MKT1* into another leucine codon (CTa in the mkt1-D30G-2 primer). While preserving the amino acid sequence of the protein, this second nucleotide change introduces a new *Avr*II restriction site (boxed) in this *MKT1-30G* allele to simplify genotyping. The insert in pRS306-*MKT1*-D30G was sequence verified and contains only these two additional nucleotide changes compared to the S288C sequence of *MKT1*.

Allelic replacement details: The *SAL1* and *CAT5* allelic replacements were executed by two sequential transformations as described in detail elsewhere (GRAY *et al.* 2004). Briefly, the first transformation integrates the *URA3* marker into the targeted locus (*sal1-1* or *CAT5-91I*). The second transformation replaces *URA3* with a PCR product, which in our case was amplified from RM11-1a genomic DNA.

For the replacement of the *sal1-1* allele, the PCR product was generated with primers *SAL1*_F2 (TTTACCTATTCAACGAAGATGTCG) and *SAL1*_R2 (AGCTGATGGAAACTGCTGGA). The RM11-1a sequence between these two primers differs from the S288C sequence only in the stretch 5'-GGTGGGCTC-3' for codons 401 through 403 in RM11-1a versus 5'-GGGGGGGGTC-3' in S288C (Figure 6A). Thus, in addition to reverting the frameshift mutation in S288C, our allele replacement also introduces a different codon for the glycine amino acid in the 401st position of Sal1p (GGT in RM11 versus GGG in S288C).

For the replacement of the *CAT5-91I* allele, the PCR product was generated with primers *CAT5*_F (GCAGAGGCTTTTCCGTCTTA) and i*CAT5*_R (TTTATCAAACCGTTTTCCTTTCA). The RM11-1a sequence between these two primers differs from the S288C sequence at only three nucleotides. Only one is a non-synonymous SNP that changes the amino acid at the 91st position of the Cat1p (Figure 6C). The other two are silent SNPs that do not change the amino acid sequence of the protein. Interestingly, these two silent SNPs cluster very closely to the 91st amino acid position – one alters the 85th codon for lysine (AAA in S288C versus AAG in RM11-a, the other alters the 89th codon for lysine (AAG in S288C versus AAA in RM11-1a). Therefore, our *CAT5* allele replacement changes the only amino acid difference between the S288C and RM11-1a Cat5p, namely the one at the 91st position (Figure 6C).

Colony counting by ImageJ: In order to count *petite* and *grande* colonies with ImageJ, YEPDG plates were scanned as a transparency with an Epson Expression 1680 scanner and SF Launcher v.2.1.0 software. The scan resolution was 300 dots per inch without a filter to generate a 16→8 bit greyscale tiff file, which was manipulated further in ImageJ. Using the "MultiThresholder" plug-in filter in ImageJ, the tiff files were converted to black and white, binary images. The "Watershed" function was run consecutively twice to maximize the separation of merged colonies. The "Analyze Particles" function was then used to count the colonies. The use of BD Falcon, 150x15mm plates (catalog number 35 1058) allowed us to apply the "Analyze Particles" function to the entire area of a plate because these plates do not contain additional edges on the bottom. The settings for the "Analyze Particles" function were: size (in pixels) between 5 and infinity; circularity between 0.60 and 1.00; excluding colonies that lay on the edges of the analyzed area. The "Analyze Particles" function returns data on the size of each colony and the total number of colonies. To count the number of *petite* colonies, the distribution of colony size was generated and a cut-off pixel size that readily distinguished

between small and large colonies was determined. That cut-off was used to count the number of *petite* colonies. In optimizing this protocol, we determined that the correlation between manually versus ImageJ counted plates with a broad range of median *petite* frequencies was extremely high ($R^2 = 0.9980$, data not shown).

OD doubling time measurements: OD doubling times were measured at 660nm in 96-well plates using a Powerwave XS plate reader (BioTek, Winooski, VT) using a modification of the protocol in (TOUSSAINT and CONCONI 2006; VEATCH *et al.* 2009). To follow the growth rate of the same culture for a long period of time, a series of seven four-fold dilutions of each original culture were made in final volumes of 100µl. The plates were grown at 30° with high, continuous shaking for 48 hours with absorbance reads every 10 minutes. OD doubling times of individual wells were calculated for values of the path-length-unadjusted absorbance between 0.0625 and 0.25. The OD doubling time was calculated by linear regression of the $\log_2$ transformed ODs using all data points within this specified range. Each strain was analyzed in biological triplicate.

Literature Cited for Supporting Materials & Methods

GRAY, M., M. KUPIEC and S. M. HONIGBERG, 2004 Site-specific genomic (SSG) and random domain-localized (RDL) mutagenesis in yeast. BMC Biotechnol **4:** 7.

SIKORSKI, R. S., and P. HIETER, 1989 A system of shuttle vectors and yeast host strains designed for efficient manipulation of DNA in Saccharomyces cerevisiae. Genetics **122:** 19-27.

TOUSSAINT, M., and A. CONCONI, 2006 High-throughput and sensitive assay to measure yeast cell growth: a bench protocol for testing genotoxic agents. Nat Protoc **1:** 1922-1928.

VEATCH, J. R., M. A. MCMURRAY, Z. W. NELSON and D. E. GOTTSCHLING, 2009 Mitochondrial dysfunction leads to nuclear genome instability: A link through iron-sulfur clusters. Cell**:** in press.

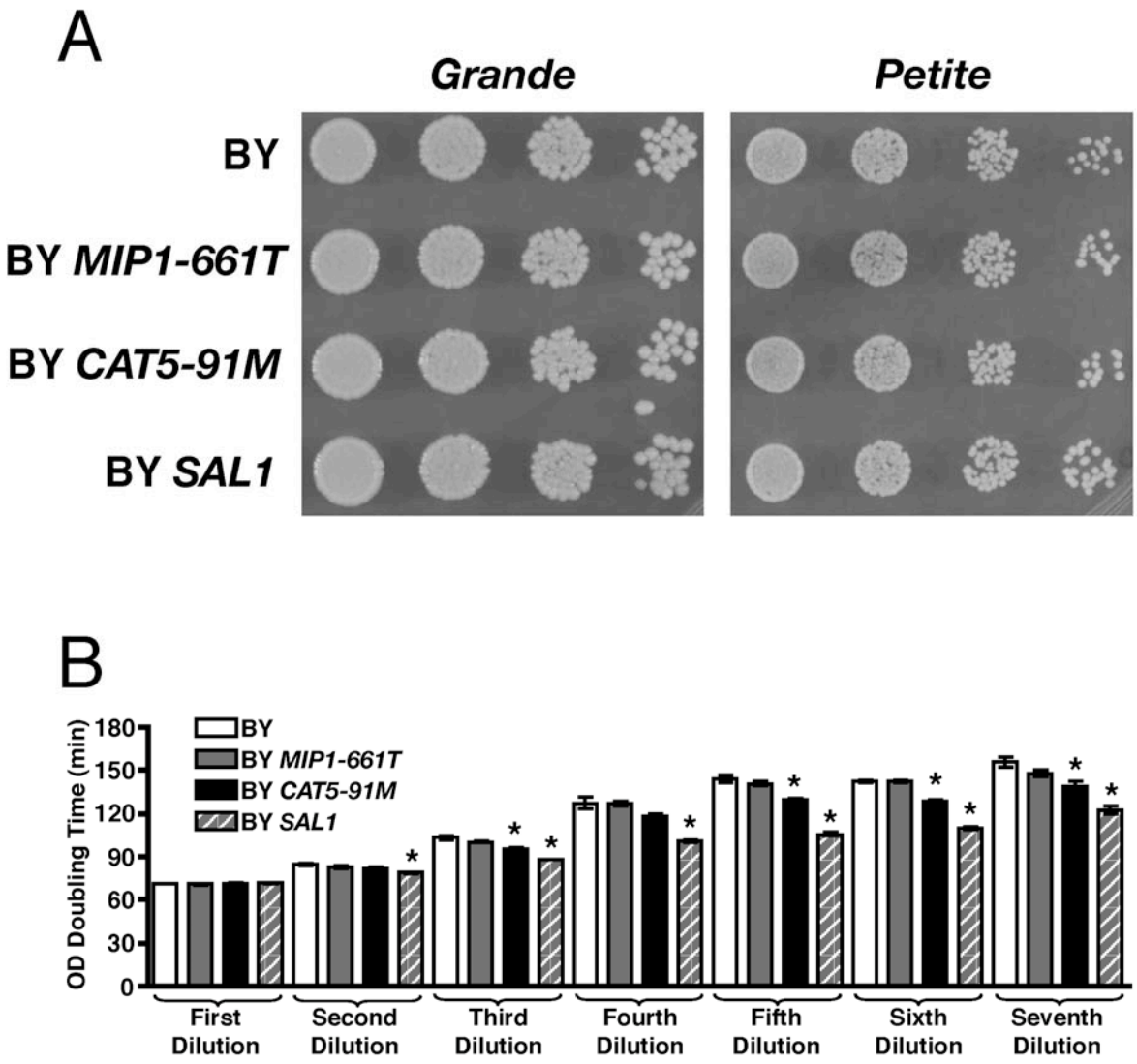

FIGURE S1.—The BY alleles of *SAL1*, *CAT5*, and *MIP1* do not affect growth of *petite*s. (A) Serial dilutions of *grande* (left) and *petite* (right) cells (see Materials & Methods) of the strains UCC8356, UCC8357, UCC8358, and UCC8360 were applied to YEPD plates. (B) Cultures of *petite* cells from the strains in (A) were generated as described in the Materials & Methods. Seven four-fold serial dilutions of each culture were analyzed in a Powerwave XS plate reader as described in Supporting Materials & Methods. Each bar represents the mean of three biological replicates for that strain. The error bars represent one standard error of the mean. The asterisks denote a statistically significant decrease (p-value < 0.05) in OD doubling time of the strain compared to the BY reference strain (UCC8356) in that particular dilution.

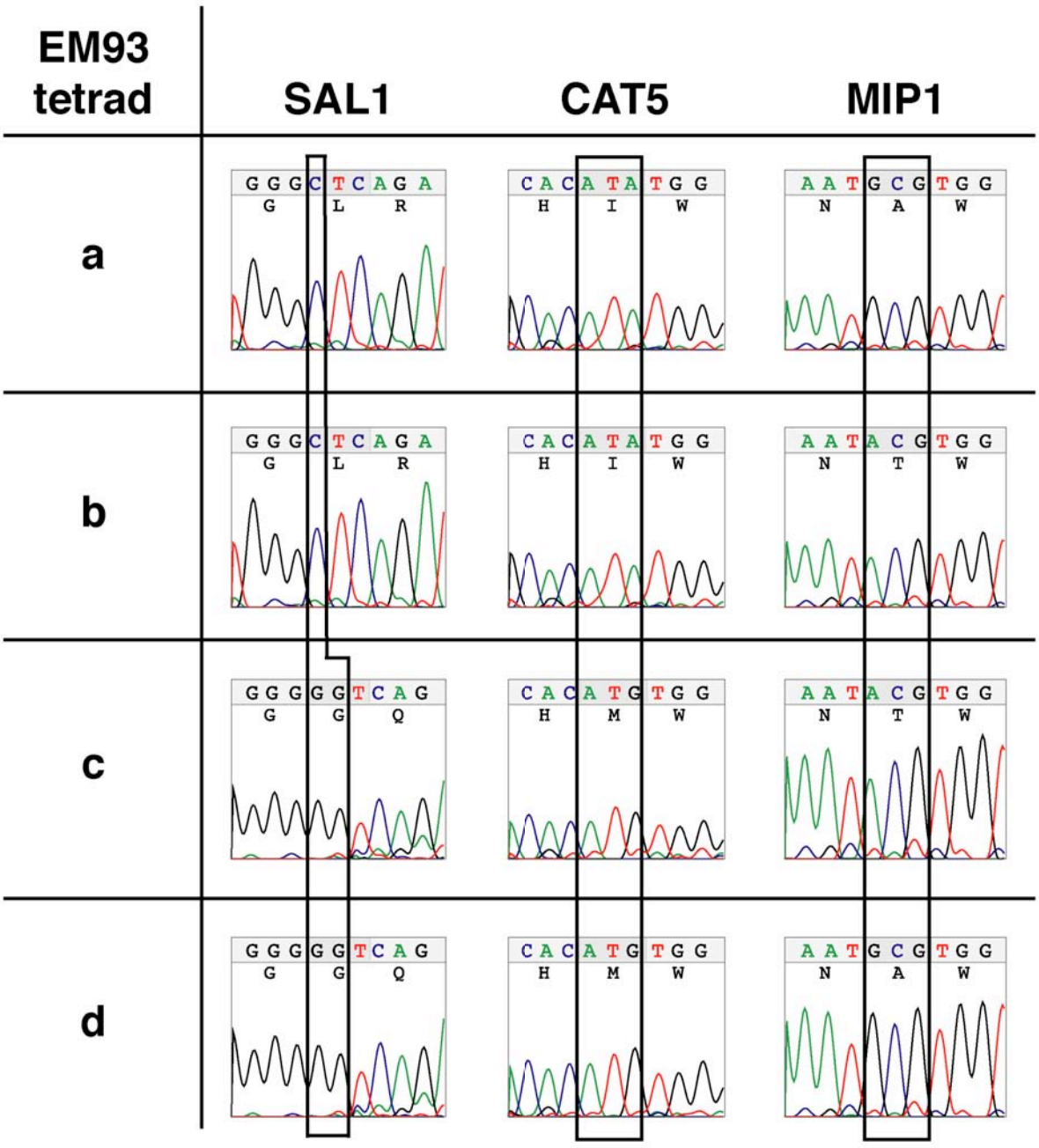

FIGURE S2.—EM93 is the source of the BY/S288C *sal1-1*, *CAT5-91I*, and *MIP1-661A* alleles. The diploid EM93 strain was sporulated. Each spore of a tetrad was sequenced for a region encompassing the relevant polymorphisms in the *SAL1*, *CAT5*, and *MIP1* genes. Each trace picture shows the relevant DNA (top) and protein (underneath) sequence. The black box in the *SAL1* column highlights the heterozygosity of the *sal1-1* frameshift mutation (present in spores c & d). The amino acid differences in *CAT5* and *MIP1* are also boxed in black.

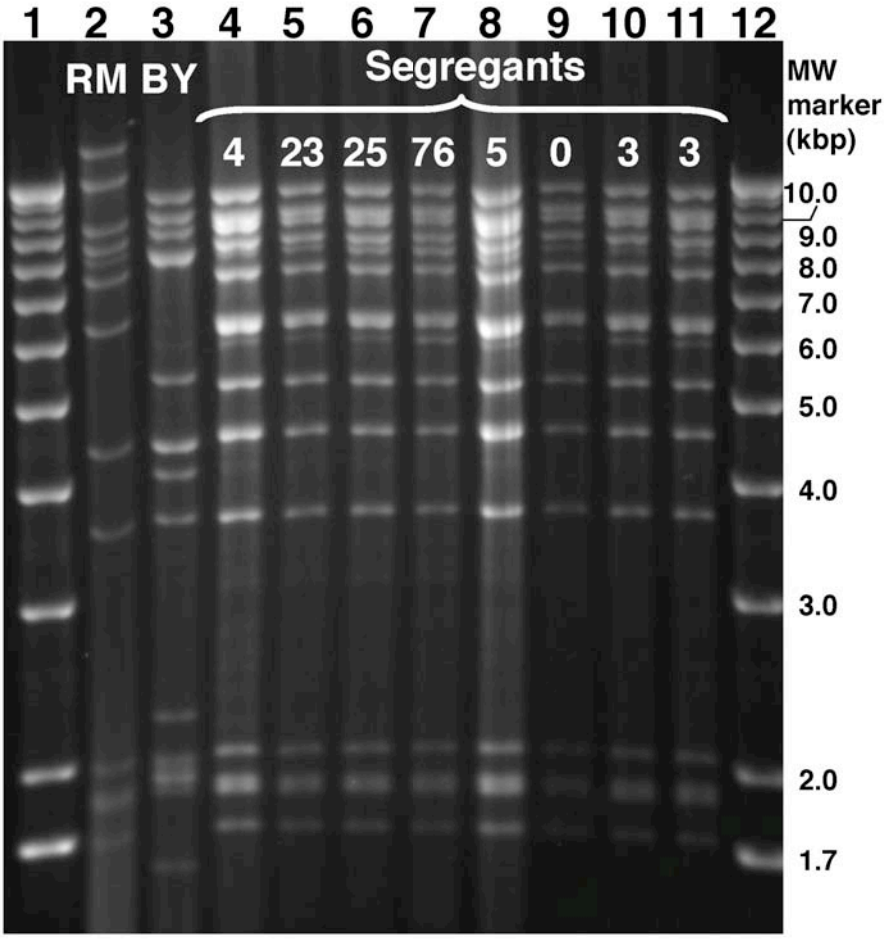

FIGURE S3.—Segregants of the BY x RM cross all have identical mtDNA, which is a recombinant version of the BY and RM mtDNAs. mtDNA was isolated from the two parents – BY4716 & RM11-1a, as well as from 8 segregants from the BY x RM cross whose median *petite* frequencies varied within a large range (indicated as a white number at the top of the lane). The mtDNA was digested with *Eco*RV and run out on a 0.6% agarose gel. Lanes 1 and 12 contain DNA size markers. Lane 2 and 3 contain the digested mtDNA of the RM11-1a and BY4716 parent, respectively. Lanes 4 through 11 contain the digested mtDNA of the 8 segregants.

TABLE S1

PCR and sequencing primers

Primer name	Sequence	Comments
MKT1_F2	TGGTGGAAAATCTGGAAAGC	Use with MKT1_R to PCR amplify and sequence the *MKT1-30G* or *MKT1-30D* allele
MKT1_R	TTCCATTGTGTCCAGCCTCT	See comments for MKT1_F2
SAL1_F	GGCTTTTTATGTTGGGAACG	Use with SAL1_R to PCR amplify and sequence the *sal1-1* or wild-type allele of *SAL1*
SAL1_R	GCATATGTTCCTTGGGCTTG	See comments for SAL1_F
CAT5_F2	CCTCCAAACCAATTCAAGGA	Use with iCAT5_R2 to PCR amplify the *CAT5* genomic locus. The PCR product is to be sequenced with CAT5_F to distinguish between the *CAT5-91M* and *CAT5-91I* allele
iCAT5_R2	TGAACCCATACCCCATTTACA	See comments for CAT5_F2
CAT5_F	GCAGAGGCTTTTCCGTCTTA	Use to sequence the PCR product generated with CAT5-F2 and iCAT5_R2
MIP1_F0	GGTGTTCCTGCAAAGTGTCA	Use with MIP1_R to sequence the *MIP1-661T* or *MIP1-661A* allele
MIP1_R	TTTGAGCAGTCTTCGTGTGC	See comments for MIP1_F0
COX1_A1_F	GGTATGGCAGGAACAGCAAT	Use with COX1_A2_R to check for the absence of intron aI1 in *COX1* in RM
COX1_A2_R	AGAAAATCATTAATACAGCATGACC AACTACTAAAA	See notes for COX1_A1_F
COX1_A5a_F	TGCTATGGCTTCAATTGGATT	Use with COX1_A6_R to check for the absence of introns aI5a, aI5b and aI5c in *COX1* in RM
COX1_A6_R	ATTTCATCCTGCGAAAGCAT	See notes to COX1_A5a_F
21S_rRNA_F	AGGTGTGAACCCCTCTTCG	Use with 21S_rRNA_R to check for the absence of the r1 (omega) intron in RM
21S_rRNA_R	CCATGGGTTGATTCATTATGG	See notes for 21S_rRNA_F
COX1_aI1_F	GCACAGGCAGTGTGAAAAAG	Use with COX1_aI1_R to confirm presence of intron aI1 in *COX1* in BY
COX1_aI1_R	TCTAAAACCATGTGAATGTGTTGA	See notes for COX1_aI1_F
COX1_aI5a_F	AAATCCCTTTAGCAAGGATAAAAA	Use with COX1_aI5a_R to confirm presence of intron aI5a in *COX1* in BY
COX1_aI5a_R	TCCACCTTTTACAAATGAACCA	See notes for COX1_aI5a_F
COX1_aI5b_F	GGCCCCCGAAACTAAAGATA	Use with COX1_aI5b_R to confirm presence of intron aI5b in *COX1* in BY
COX1_aI5b_R	CGGGCCGGACTAAAATATAA	See notes for COX1_aI5b_F
COX1_aI5c_F	TGCTCAACGAAAGTGAATCAA	Use with COX1_aI5c_R to confirm presence of intron aI5c in *COX1* in BY
COX1_aI5c_R	ACAAGTTTTCCCCCGGTAAG	See notes for COX1_aI5c_F
omega_F	ATTTACCCCCTTGTCCCATT	Use with omega_R to confirm presence of r1(omega) intron in BY
omega_R	CCAATACCTGCTTCAAATTGTTC	See notes for omega_F